

Compressive Sampling using Annihilating Filter-based Low-Rank Interpolation

Jong Chul Ye *Senior Member, IEEE*, Jong Min Kim, and Kyong Hwan Jin

Abstract

While the recent theory of compressed sensing or compressive sampling (CS) provides an opportunity to overcome the Nyquist limit in recovering sparse signals, a recovery algorithm usually takes the form of penalized least squares or constraint optimization framework that is different from classical signal sampling theory. In this paper, we provide a drastically different compressive sampling framework that can exploit all the benefits of the CS, but can be still implemented in a classical sampling framework using a digital correction filter. The main idea is originated from the fundamental duality between the sparsity in the primary space and the low-rankness of a structured matrix in the reciprocal spaces, which demonstrates that the low-rank interpolator as a digital correction filter can enjoy all the optimality of the standard CS. We show that the idea can be generalised to recover signals in large class of signals such as piece-wise polynomial, and spline representations. Moreover, by restricting signal class as cardinal splines, the proposed low-rank interpolation approach can achieve inherent regularization to improve the noise robustness. Using the powerful dual certificates and golfing scheme by Gross, we show that the new framework still achieves the near-optimal sampling rate for signal recovery. Numerical results using various type of signals confirmed that the proposed scheme has significant better phase transition than the conventional CS approaches.

Index Terms

Sampling theory, compressed sensing, signals of finite rate of innovations, low rank matrix completion, structured matrix, piecewise polynomials, non-uniform splines, cardinal splines, dual certificates, golfing scheme

Correspondence to:

Jong Chul Ye, Ph.D

Professor

Department of Bio and Brain Engineering

Korea Adv. Inst. of Science and Technology (KAIST)

373-1 Guseong-Dong, Yuseong-Gu, Daejeon 305-701, Korea

Tel: +82-42-350-4320

Email: jong.ye@kaist.ac.kr

I. INTRODUCTION

Compressed sensing or compressive sampling (CS) theory [1]–[3] addresses the accurate recovery of unknown sparse signals from underdetermined linear measurements. Most of the compressive sensing theories have been developed to address recovery problems from discrete measurements [1]–[3]. More specifically, let m and n be positive integers such that $m < n$. Then, the compressed sensing problem is formulated as

$$(P0) : \quad \begin{aligned} & \text{minimize} \quad \|\mathbf{x}\|_0 \\ & \text{subject to} \quad \mathbf{b} = A\mathbf{x}, \end{aligned} \quad (1)$$

where $\mathbf{b} \in \mathbb{R}^m$, $A \in \mathbb{R}^{m \times n}$, $\mathbf{x} \in \mathbb{R}^n$, and $\|\mathbf{x}\|_0 = r$ denotes the number of non-zero elements in the vector \mathbf{x} . In particular, Fourier compressive sampling problems, where the sensing matrix A comes from sub-sampled Fourier matrix, have many important applications in imaging and signal analysis.

Even though the original underdetermined linear equation $\mathbf{y} = A\mathbf{x}$ has infinitely many solutions, the compressed sensing theory says that if r is sufficiently small or \mathbf{x} is *sparse*, then there exists the unique solution for (1). One of the important theoretical tools that guarantees the unique recovery is so-called restricted isometry property (RIP) [3]. More specifically, a sensing matrix $A \in \mathbb{R}^{m \times n}$ is said to have a r -restricted isometry property (RIP) if there is a constant $0 \leq \delta_r < 1$ such that

$$(1 - \delta_r)\|\mathbf{x}\|^2 \leq \|A\mathbf{x}\|^2 \leq (1 + \delta_r)\|\mathbf{x}\|^2$$

for all $\mathbf{x} \in \mathbb{R}^n$ such that $\|\mathbf{x}\|_0 \leq r$. It was demonstrated that $\delta_{2r} < \sqrt{2} - 1$ is sufficient for unique recovery when we convert (1) into a more feasible l_1 convex problem [2]. For many classes of random matrices, the RIP condition is satisfied with high probability if the number of measurements satisfies $m \geq cr \log(n/r)$ for some constant $c > 0$ [3]. To address the resulting sparse recovery problem, greedy methods [4], reweighted norm algorithms [5], [6], convex relaxation using l_1 norm [2], [7], or Bayesian approaches [8], [9] have been widely investigated as alternatives. Most of these recovery algorithms require iterative applications of forward A and its adjoint A^* operators, and efficient implementations using modern convex optimization tools such as proximal optimization have become very extensive research topics [10].

On the other hand, there exist another type of compressive sampling approaches for the signals with finite rate of innovations (FRI) [11]–[13]. An important example of continuous signals with the finite rate of innovation is a periodic stream of Diracs [11]:

$$x(t) = \sum_{l \in \mathbb{Z}} \sum_{i=0}^{r-1} c_i \delta(t - t_i - l\tau), \quad (2)$$

where $c_{l+r} = c_l, \forall l \in \mathbb{Z}$. This signals has $2r$ degrees of freedom for each period, so by introducing a counting function $C_x(t_a, t_b)$ that counts the number of degrees of freedom of $x(t)$ within $[t_a, t_b]$, the rate of innovation ρ

can be shown as

$$\rho = \lim_{\tau \rightarrow \infty} \frac{1}{\tau} C_x(0, \tau) = \frac{2r}{\tau}. \quad (3)$$

Since the finite rate of innovation implies the sparseness of the underlying signals, there must be a way of sampling a FRI signal $x(t)$ much more efficiently compared to the standard Nyquist sampling. In fact, this has been another active areas of research in modern sampling theory, and the standard approach to address this problem is using annihilating filters and polynomial root finding [11]–[13]. It is now well-known that the sampling rate that matches the rate of innovation is sufficient for recovery of underlying signals [11]–[13].

While both compressed sensing and the FRI sampling theory deal with compressive sampling, there exist technical differences between the two approaches, as discussed in a recent review article [14]. First, the compressed sensing theory deals with signal recovery in a discrete setup, whereas the FRI sampling theory is concerned about continuous signal recovery. Second, FRI sampling theory addresses the time domain sampling, so it was mainly developed under the uniform sampling scheme, whereas a random sampling scheme is essential for the analysis of compressed sensing. Last, but not the least, important distinction between the two approaches is their recovery algorithms. In most of the compressive sensing approaches, sparsity constrained optimization or penalized least squares is used, whereas the polynomial root finding is one of the major approaches for FRI sampling theory.

In fact, overcoming the “discrete” limitation of compressed sensing has been an active area of researches in recent years [15]–[18] and, as an example, so-called *spectral compressed sensing* using structured matrix completion has been recently proposed [18]. More specifically, Chen and Chi [18] dealt with the recovery of spikes using data in the spectral domain. For example, a spectral measurement at ω is given by a weighted sum of complex sinusoids at r distinct frequencies $\{\omega_j \in [0, 2\pi] : 0 \leq j \leq r-1\}$:

$$\hat{x}(\omega) = \sum_{j=0}^{r-1} c_j e^{-i\omega_j t_j}. \quad (4)$$

By constructing a high dimensional Hankel structured matrix and imposing a low rankness, Chen and Chi [18] recovered fully sampled spectral data first, after which a matrix pencil approach was used to identify the location of the peaks. Using the beautiful tools of dual certificate and the so-called “golfing scheme” originally developed by Gross [19], they showed that $m \geq \mathcal{O}(r \log^4 n)$ random samples in n -dimensional ambient space guarantees the robust recovery with a high probability [18].

The discovery of continuous domain compressed sensing now leads to a natural question: is there any equivalence relationship between the spectral compressed sensing and the sampling theory of FRI signals? In fact, this links have been implied by many authors, and one of the important contributions of the present work is to confirm that spectral compressed sensing is indeed equivalent to the FRI sampling theory for Diracs with the help of structured matrix completion; moreover, it can be generalised to develop a unified Fourier compressive sampling theory for large class of signals such as piece-wise polynomials, splines or so on. Interestingly, the resulting Fourier compressed sensing formulation can be reduced to a spectral domain interpolation problem that can be implemented using a *low-rank interpolator*, which is implemented through a *weighted* structured matrix completion. We can further showed that

such conversion to a spectral interpolation problem does not lose any optimality, because the required sampling rate for accurate recovery is still $m \geq \mathcal{O}(r \log^2 n)$, which is as good as most of the Fourier compressed sensing results. Furthermore, this is an improvement over the $\mathcal{O}(r \log^4 n)$ result by Chen and Chi [18]. Another important contribution is that by restricting the signal class to cardinal splines, the proposed low-rank interpolation provides a natural regularization that can restrict noise boosting from recovering infinitesimal resolution FRI signals.

Note that the proposed approach is fundamentally different from classical compressed sensing approaches, which regard a sampling problem as an inverse problem (see Eq. (1)). In fact, the proposed approach is more closely related to the classical sampling theory, where signal sampling block is decoupled from a signal recovery block. For example, in general sampling theory for signals in the shift-invariant spaces [20], [21], the nature of the signal representation in a shift invariant space can be fully taken care of as a *digital correction filter*, after which signal recovery is performed by convolution with a reconstruction filter (see Fig. 1(a)). However, the introduction of the compressed sensing theory has totally changed this classical picture, because of a feedback scheme as shown in Fig. 1(b). More specifically, in CS, the signal sampling is mixed together with the signal recovery through a feedback loop, so CS requires iterative applications of signal sampling and recovery as shown in Fig. 1(b). On the other hand, by introducing a *low rank interpolator* as a digital correction filter, the proposed scheme is more similar to the traditional sampling as shown in Fig. 1(c).

The elimination of the feedback loop is important, because the proposed low rank interpolator can be implemented as a preprocessing block in front of a classical signal processing pipeline, which makes the implementation very practical. In spite of the proposed simplification, we can still prove that the low rank interpolation step enjoys all the benefit of exploiting the sparsity as in the standard compressed sensing, and sometimes it has many advantages over the standard penalized least squares framework of CS. The superior performance of the low-rank interpolation scheme over standard CS has been demonstrated in various biomedical imaging and image processing applications such as magnetic resonance imaging (MRI) [22], [23], image inpainting [24], super-resolution microscopy [25], image denoising [26], and so on, which clearly confirm the practicality of the new theory.

This paper consists of followings. Section II explains the FRI sampling theory and provides its links to spectral compressed sensing problems. Section III then discussed the proposed low-rank interpolation theory for recovery of various type of signals. Fundamental sampling rates for accurate and stable recovery are given in section IV. Section V explains algorithmic implementation. Numerical results are then provided in Section VI, which is followed by conclusion in Section VII.

II. LINK BETWEEN FRI SAMPLING AND SPECTRAL COMPRESSED SENSING

A. Notations and Mathematical Preliminaries

Throughout this paper, \mathbf{x}^i and \mathbf{x}_j correspond to the i -th row and the j -th column of matrix X , respectively. The (i, j) element of X is represented by x_{ij} . When S is an index set of a matrix elements, A_S correspond to a submatrix collecting corresponding the index set S . For a matrix A , $\text{Tr}(A)$ is the trace of a matrix A ; A^* is its adjoint; A^\dagger denotes the Penrose-Moor pseudo-inverse. A Hankel structured matrix generated from a n -dimensional

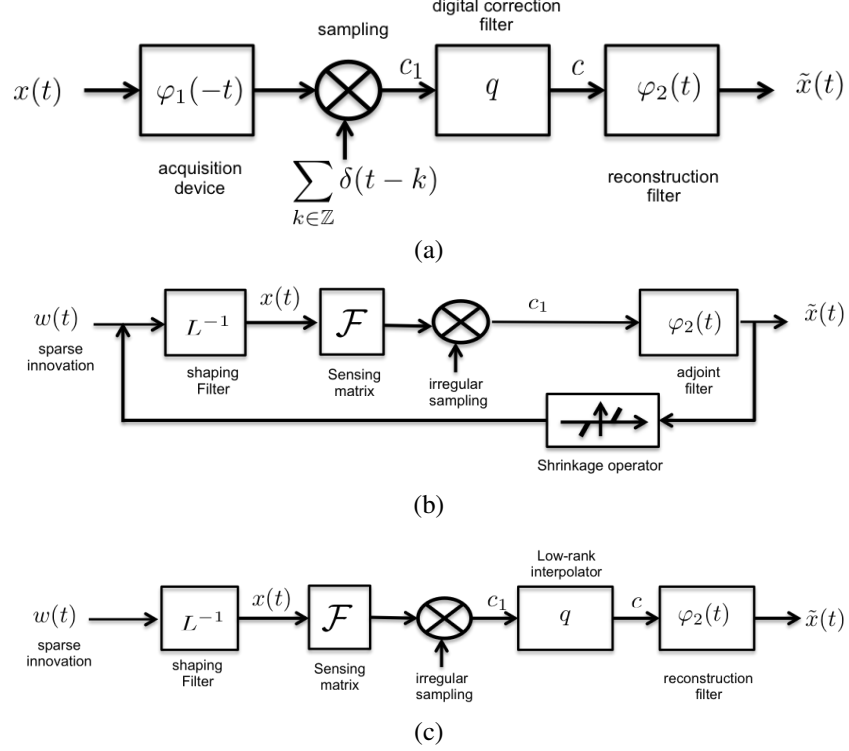


Fig. 1. Comparison with various sampling schemes. (a) Generalized sampling [20], [21]: here, a continuous input signal is filtered through a acquisition device, after which uniform sampling is performed. The goal of sampling is to impose consistency condition such that if the reconstructed signal is used as an input to the acquisition device, it can generate the same discrete sequence $\{c_1\}$. This can be taken care of by the digital correction filter q . (b) Compressed sensing: here, the continuous signal $x(t)$ can be generated from sparse innovation $w(t)$ through a shaping filter L^{-1} [27], [28], and its measurement through a sensing matrix are irregularly sampled. The reconstruction is performed in an iterative manner using a shrinkage operator. (c) Proposed sampling scheme: Here, the iterative reconstruction framework in CS is replaced by a discrete low-rank interpolator, and the final reconstruction is obtained using the reconstruction filter from fully sampled data.

vector $\mathbf{x} = [x[0], \dots, x[n-1]]^T \in \mathbb{C}^n$ has the following structure:

$$\mathcal{H}(\mathbf{x}) = \begin{bmatrix} x[0] & x[1] & \cdots & x[d-1] \\ x[1] & x[2] & \cdots & x[d] \\ \vdots & \vdots & \ddots & \vdots \\ x[n-d] & [n-d+1] & \cdots & x[n-1] \end{bmatrix} \in \mathbb{C}^{(n-d+1) \times d}. \quad (5)$$

where d is called a matrix pencil parameter. We denote the space of this type of Hankel structure matrices as $\mathcal{H}(n, d)$.

A $n \times d$ circulant matrix generated from a n -dimensional vector $\mathbf{u} = [u[0], \dots, u[n-1]]^T \in \mathbb{C}^n$ has the following

structure:

$$\mathcal{H}_c(\hat{\mathbf{u}}) = \begin{bmatrix} \hat{u}[0] & \hat{u}[1] & \cdots & \hat{u}[d-1] \\ \hat{u}[1] & \hat{u}[2] & \cdots & \hat{u}[d] \\ \vdots & \vdots & \ddots & \vdots \\ \hat{u}[n-d] & \hat{u}[n-d+1] & \cdots & \hat{u}[n-1] \\ \hline \hat{u}[n-d+1] & \hat{u}[n-d+2] & \cdots & \hat{u}[0] \\ \vdots & \vdots & \ddots & \vdots \\ \hat{u}[n-1] & \hat{u}[0] & \cdots & \hat{u}[d-2] \end{bmatrix} \in \mathbb{C}^{n \times d}. \quad (6)$$

Note that $n \times d$ circulant matrix can be considered as a Hankel matrix of $(d-1)$ -element augmented vector from $\mathbf{u} \in \mathbb{C}^n$ with the periodic boundary expansion:

$$\tilde{\mathbf{u}} = \begin{bmatrix} \mathbf{u}^T & \underbrace{u[0] \ u[1] \ \cdots \ u[d-2]}_{(d-1)} \end{bmatrix}^T \in \mathbb{C}^{n+d-1}.$$

We denote the space of this type of circulant structure matrices as $\mathcal{H}_c(n, d)$.

Let A be a $n \times n_2$ matrix with rank r . The following matrix norm inequalities are useful

$$\|A\| \leq \|A\|_F \leq \|A\|_* \leq \sqrt{r}\|A\|_F \leq \sqrt{r}\|A\| \quad (7)$$

$$\|A\|_\infty \leq \|A\| \leq \sqrt{nn_2}\|A\|_\infty \quad (8)$$

where $\|A\|_\infty = \max_{i,j} |a_{ij}|$ and $\|A\|$, $\|A\|_F$ and $\|A\|_*$ denote the spectral norm, Frobenius norm, and the nuclear norm, respectively. We define matrix inner product for the matrix A and B :

$$\langle A, B \rangle = \text{Tr}(A^* B).$$

Then, for any given matrix norm, we can define a dual norm:

$$\|X\|_d = \max_Y \{ \langle X, Y \rangle : \|Y\| \leq 1 \}.$$

Note that the dual norm of Frobenius norm is the Frobenius norm, and the dual norm of the spectral norm is the nuclear norm. We often use the following matrix inequalities:

$$\langle W, H \rangle := \text{Tr}(W^* H) \leq \|W\|_F \|H\|_F \quad (9)$$

$$\langle W, H \rangle \leq \|W\| \|H\|_*, \quad (10)$$

$$\langle W, H \rangle \leq \|W\|_\infty \|H\|_*, \quad (11)$$

where the first one comes from Cauchy-Schwartz inequality, and the last inequality is known as *trace duality* property.

B. Review of FRI Sampling Theory

Consider the periodic stream of Diracs in (2). This can be written as

$$\begin{aligned}
 x(t) &= \sum_{j=0}^{r-1} c_j \sum_{l \in \mathbb{Z}} \delta(t - t_j - l\tau) \\
 &= \sum_{j=0}^{r-1} c_j \frac{1}{\tau} \sum_{l \in \mathbb{Z}} e^{i(2\pi l(t-t_j)/\tau)} \\
 &= \sum_{n \in \mathbb{Z}} \hat{x}[l] e^{i2\pi lt/\tau}
 \end{aligned}$$

where the Fourier series coefficient $\hat{x}[l]$ is given by

$$\hat{x}[l] = \frac{1}{\tau} \sum_{j=0}^{r-1} c_j e^{-i2\pi t_j l/\tau} . \quad (12)$$

If we construct a filter $\hat{h}[l]$ that has the following z-transform representation:

$$\hat{h}(z) = \sum_{l=0}^r \hat{h}[l] z^{-l} = \prod_{j=0}^{r-1} (1 - e^{-i2\pi t_j/\tau} z^{-1}) , \quad (13)$$

then it annihilates the signal $\hat{x}[l]$, because

$$\begin{aligned}
 (\hat{h} * \hat{x})[l] &= \sum_{p=0}^k \hat{h}[p] \hat{x}[l-p] \\
 &= \sum_{p=0}^r \sum_{j=0}^{r-1} c_j \hat{h}[p] u_j^{l-p} \\
 &= \sum_{j=0}^{r-1} c_j \underbrace{\left(\sum_{p=0}^r \hat{h}[p] u_j^{-p} \right)}_{\hat{h}(u_j)} u_j^l = 0
 \end{aligned} \quad (14)$$

where $u_j = e^{-i2\pi t_j/\tau}$. Now, define a sinc kernel with bandwidth $[-B\pi, B\pi]$ where $B \in \mathbb{R}_+$ as $q_B(t) := B \text{sinc}(Bt)$.

Then, the classic FRI sampling theorem can be stated as following [11]–[13]:

Theorem II.1. [11] Consider $x(t)$, which is a periodic stream of Diracs of period τ with r Diracs given by (2). Take a sampling kernel $q_B(t) = B \text{sinc}(Bt)$ where $B \geq \rho$, where the rate of innovation ρ is given by (3). Then, for $m \geq 2p + 1$ and $p = \lfloor B\tau/2 \rfloor \geq r$ and T is a divisor of τ , the samples

$$y_i = \langle q_B(t - iT), x(t) \rangle, \quad i = 0, \dots, m-1, \quad (15)$$

are sufficient to recover $x(t)$.

C. Spectral Compressed Sensing

The aforementioned sampling theory for stream of Diracs was developed for time domain sampling. Thus, the uniform sampling with an appropriate sampling kernel is the standard method for signal acquisition. On the other hand, in many spectral compressed sensing problems such as sensor array signal processing [29] or magnetic resonance imaging (MRI) [30], the measurement is obtained in the spectral domain, so we deal with the recovery of spectral components from their superposition measurements:

$$\hat{x}(\omega) = \sum_{j=0}^{r-1} c_j e^{-i\omega t_j}, \quad (16)$$

where $\{t_j\}_{j=0}^{r-1}$ and its coefficients $\{c_j\}_{j=0}^{r-1}$ are unknown and need to be estimated. In spectral compressed sensing, one is interested in placing the minimum number of sensors in the frequency domain to recover the time domain impulses. So, one usually restricts the antenna locations on the uniform grid in the frequency domain. In this case, to avoid aliasing artefacts, the grid size should be at most:

$$\Delta = 2\pi/\tau.$$

In this case, the frequency domain measurement can be converted to

$$\hat{x}[l] := \hat{x}(l\Delta) = \sum_{j=0}^{r-1} c_j e^{-i2\pi l t_j / \tau}, \quad m \in \Omega \quad (17)$$

where the index set Ω with $|\Omega| \ll n$ denotes the sparse sampling indices that are usually determined by random distribution.

To address the recovery problem from random sparse samples $\{\hat{x}[m]\}$, Chen and Chi [18] developed so-called *enhanced matrix completion (EMaC)* algorithm inspired by the matrix pencil approach in spectral estimation problems. Specifically, they define a spectral vector $\hat{\mathbf{x}}$:

$$\hat{\mathbf{x}} = [\hat{x}[0] \quad \cdots \quad \hat{x}[n-1]]^T \in \mathbb{C}^n \quad (18)$$

and then constructed the following enhanced matrix in Hankel structure:

$$\mathcal{H}(\hat{\mathbf{x}}) = \begin{bmatrix} \hat{x}[0] & \hat{x}[1] & \cdots & \hat{x}[d-1] \\ \hat{x}[1] & \hat{x}[2] & \cdots & \hat{x}[d] \\ \vdots & \vdots & \ddots & \vdots \\ \hat{x}[n-d] & \hat{x}[n-d+1] & \cdots & \hat{x}[n-1] \end{bmatrix} \in \mathbb{C}^{(n-d+1) \times d} \quad (19)$$

where $r \leq d \leq n$ is called a matrix pencil parameter [31]. Then, the explicit representation of $\mathcal{H}(\hat{\mathbf{x}})$ is given by [18]:

$$\mathcal{H}(\hat{\mathbf{x}}) = L D R^T \quad (20)$$

where

$$L = \begin{bmatrix} 1 & 1 & \cdots & 1 \\ y_0 & y_1 & \cdots & y_{k-1} \\ \vdots & \vdots & \ddots & \vdots \\ y_0^{n-d} & y_1^{n-d} & \cdots & y_{r-1}^{n-d} \end{bmatrix} \in \mathbb{C}^{(n-d+1) \times r} \quad (21)$$

$$R = \begin{bmatrix} 1 & 1 & \cdots & 1 \\ y_0 & y_1 & \cdots & y_{k-1} \\ \vdots & \vdots & \ddots & \vdots \\ y_0^{d-1} & y_1^{d-1} & \cdots & y_{r-1}^{d-1} \end{bmatrix} \in \mathbb{C}^{d \times r} \quad (22)$$

and

$$D = \begin{bmatrix} c_0 & 0 & \cdots & 0 \\ 0 & c_1 & \cdots & 0 \\ \vdots & \vdots & \ddots & \vdots \\ 0 & 0 & \cdots & c_{r-1} \end{bmatrix}, \quad (23)$$

and $y_j = e^{-i2\pi t_j/\tau}$ for $j = 0, \dots, r-1$. Due to the random under-sampling of $\hat{x}[m]$ on Ω , $\mathcal{H}(\hat{\mathbf{x}})$ is known only at the indices that belong to Ω . Accordingly, their goal was to find the missing matrix elements by solving the following EMaC algorithm:

$$\begin{aligned} (\text{EMaC}) \quad & \min_{\mathbf{m} \in \mathbb{C}^n} \quad \|\mathcal{H}(\mathbf{m})\|_* \\ & \text{subject to} \quad P_\Omega(\mathbf{m}) = P_\Omega(\hat{\mathbf{x}}) \end{aligned} \quad (24)$$

where $\|\cdot\|_*$ denotes the matrix nuclear norm and P_Ω is the projection operator on the sampling location Ω . After all the spectral component in the uniform grid is obtained, the actual *off-grid* spectral components can be obtained using the matrix pencil approach in the classical spectral estimation techniques [31].

Importantly, using the powerful dual certificate and golfing scheme originally developed by David Gross [19], Chen and Chi [18] derived the following performance guarantee:

Theorem II.2. [18] *Let $\hat{\mathbf{x}}$ be given by (17) and (18), and Ω the random locations set with $|\Omega| = m$. Suppose that all measurements are noiseless. Then, there exists a universal constant $c_1 > 0$ such that there exists the unique solution to EMaC in (24) with probability exceeding $1 - n^{-2}$, provided that*

$$m > c_1 \mu_1 c_s r \log^4(n) \quad (25)$$

where

$$c_s = \max\{n/d, n/(n-d+1)\}. \quad (26)$$

and μ_1 denotes the incoherence parameter.

In practice, measurements are often contaminated by a certain amount of noise such that the noisy measurement $\hat{\mathbf{y}}$ is given by

$$R_\Omega(\hat{\mathbf{y}}) = R_\Omega(\hat{\mathbf{x}}) + R_\Omega(\hat{\mathbf{z}})$$

where $R_\Omega(\hat{\mathbf{z}})$ is a noise term. If $\|R_\Omega(\hat{\mathbf{z}})\|_2 \leq \delta$ for some $\delta > 0$, to recover the unknown spectral measurement, Chen and Chi [18] solves the following noisy EMaC problem:

$$\begin{aligned} \text{(Noisy EMaC)} \quad & \min \|\mathcal{H}(\mathbf{m})\|_* \\ \text{subject to} \quad & \|R_\Omega(\hat{\mathbf{m}}) - R_\Omega(\hat{\mathbf{y}})\| \leq \delta \end{aligned} \quad (27)$$

Moreover, they provided a performance guarantee:

Theorem II.3. *Suppose $\hat{\mathbf{y}}$ is a noisy copy of $\hat{\mathbf{x}}$ that satisfies $\|P_\Omega(\hat{\mathbf{y}} - \hat{\mathbf{x}})\|_F \leq \delta$. Under the condition of Theorem II.2, the solution to noisy EMaC in (27) satisfies*

$$\|\hat{\mathbf{x}} - \mathbf{x}\|_F \leq 5n^3\delta \quad (28)$$

with probability exceeding $1 - n^2$.

D. Link between FRI Sampling and Spectral Compressed Sensing

In this section, we discuss the relationship between spectral compressed sensing and the FRI sampling theory, which is one of the important contributions of this paper. First, it is easy to show that spectral compressed sensing measurement in (16) comes from Fourier integral

$$\hat{x}(\omega) = \mathcal{F}\{x(t)\} = \int x(t)e^{-i\omega t}dt, \quad (29)$$

when the underlying signal is described by the superposition of r impulses

$$x(t) = \sum_{j=0}^{r-1} c_j \delta(t - t_j) \quad t_j \in [0, \tau]. \quad (30)$$

Next, by allowing spectral domain sampling with $\Delta = 2\pi/\tau$, the underlying signal becomes periodic streams of Diracs with the period τ , which is indeed a signal with the finite rate of innovation with the rate $\rho = 2r/\tau$. This is why (12) and (17) become identical up to a constant scaling factor.

Accordingly, the FRI sampling theory tells us that there exist *annihilating filter* $\hat{h}[l]$ such that

$$(\hat{h} * \hat{x})[l] = \sum_{p=0}^r \hat{h}[p] \hat{x}[l - p] = 0, \quad \forall l. \quad (31)$$

and the minimum annihilating filter size is $r+1$ [11]–[13]. In fact, we can consider a generalisation of the annihilating filter to allow much flexibility. Specifically, if $\hat{h}[l]$ is an annihilating filter with $r+1$ taps, then for any $k_1 \geq 1$ tap

filter $\hat{a}[l]$, it is easy to see that the following filter with $d = r + k_1$ taps is also an annihilating filter for $\hat{x}[l]$:

$$\hat{h}_a[l] = (\hat{a} * \hat{h})[l]. \quad (32)$$

Therefore, for a $d \geq r + 1$ tap annihilating filter $\hat{h}_a[l]$, the matrix representation of (31) is given by

$$\mathcal{C}(\hat{\mathbf{x}})\bar{\mathbf{h}}_a = \mathbf{0}$$

where $\bar{\mathbf{h}}_a$ denotes a vector that reverses the order of the elements in

$$\mathbf{h}_a = [\hat{h}_a[0], \dots, \hat{h}_a[d-1]]^T, \quad (33)$$

and

$$\mathcal{C}(\hat{\mathbf{x}}) = \begin{bmatrix} \vdots & \vdots & \ddots & \vdots \\ \hat{x}[-1] & \hat{x}[0] & \cdots & \hat{x}[d-2] \\ \hline \hat{x}[0] & \hat{x}[1] & \cdots & \hat{x}[d-1] \\ \hat{x}[1] & \hat{x}[2] & \cdots & \hat{x}[d] \\ \vdots & \vdots & \ddots & \vdots \\ \hat{x}[n-d] & \hat{x}[n-d+1] & \cdots & \hat{x}[n-1] \\ \hline \hat{x}[n-d+1] & \hat{x}[n-d+2] & \cdots & \hat{x}[n] \\ \vdots & \vdots & \ddots & \vdots \end{bmatrix} \quad (34)$$

Accordingly, by choosing n such that $n - d + 1 \geq r$ and removing the boundary data outside of the sample indices $[0, \dots, n-1]$, we can construct the following matrix equation:

$$\mathcal{H}(\hat{\mathbf{x}})\bar{\mathbf{h}}_a = \mathbf{0}, \quad (35)$$

where the Hankel structure matrix $\mathcal{H}(\hat{\mathbf{x}}) \in \mathbb{C}^{(n-d+1) \times d}$ is constructed as

$$\mathcal{H}(\hat{\mathbf{x}}) = \begin{bmatrix} \hat{x}[0] & \hat{x}[1] & \cdots & \hat{x}[d-1] \\ \hat{x}[1] & \hat{x}[2] & \cdots & \hat{x}[d] \\ \vdots & \vdots & \ddots & \vdots \\ \hat{x}[n-d] & \hat{x}[n-d+1] & \cdots & \hat{x}[n-1] \end{bmatrix} \quad (36)$$

Note that the matrix pencil parameter for Hankel structured matrix is equivalent to the annihilating filter size for the case of general FRI signals. Now, for sufficiently large annihilating filter size, we can show that the Hankel matrix is low-ranked.

Proposition II.4. *Let $r + 1$ denotes the minimum size of annihilating filters that annihilates $\hat{x}[l]$ in (31). Suppose, furthermore, d is given by $d \geq r + 1$. Then, for a given Hankel structured matrix $\mathcal{H}(\hat{\mathbf{x}}) \in \mathcal{H}(n, d)$ in (36), we*

have

$$\text{RANK} \mathcal{H}(\hat{\mathbf{x}}) \leq r, \quad (37)$$

where $\text{RANK}(\cdot)$ denotes a matrix rank.

Proof. Let $\hat{\mathbf{h}} \in \mathbb{C}^r$ be the minimum size annihilating filter. Then, (33) can be represented as

$$\hat{\mathbf{h}}_a = \mathcal{C}(\hat{\mathbf{h}})\hat{\mathbf{a}} \quad (38)$$

where $\hat{\mathbf{a}} = [\hat{a}[0] \ \cdots \ \hat{a}[k_1 - 1]]$ and $\mathcal{C}(\hat{\mathbf{h}}) \in \mathbb{C}^{d \times k_1}$ is a Toeplitz structured convolution matrix from $\hat{\mathbf{h}}$:

$$\mathcal{C}(\hat{\mathbf{h}}) = \begin{bmatrix} \hat{h}[0] & 0 & \cdots & 0 \\ \hat{h}[1] & \hat{h}[0] & \cdots & 0 \\ \vdots & \vdots & \ddots & \vdots \\ \hat{h}[r-1] & \hat{h}[r-2] & \cdots & \hat{h}[r-k_1] \\ \vdots & \vdots & \ddots & \vdots \\ 0 & 0 & \cdots & \hat{h}[r-1] \end{bmatrix} \in \mathbb{C}^{d \times k_1} \quad (39)$$

where $d = r + k_1$. Since $\mathcal{C}(\hat{\mathbf{h}})$ is a convolution matrix, it is full ranked and we can show that

$$\dim \mathcal{C}(\hat{\mathbf{h}}) = k_1,$$

where $\dim(\cdot)$ denotes the dimension of a matrix. Moreover, the range space of $\mathcal{C}(\hat{\mathbf{h}})$ now belongs to the null space of the Hankel matrix, so it is easy to show

$$k_1 = \dim \mathcal{C}(\hat{\mathbf{h}}) \leq \dim \text{NUL} \mathcal{H}(\hat{\mathbf{x}}),$$

where $\text{NUL}(\cdot)$ represent a null space of a matrix. Thus,

$$\text{RANK} \mathcal{H}(\hat{\mathbf{x}}) = \min\{d, n - d + 1\} - \dim \text{NUL} \mathcal{H}(\hat{\mathbf{x}}) \leq d - k_1 = r.$$

Q.E.D. □

Corollary II.5. *Under the condition of Proposition II.4, assume that $n - d + 1 \geq r + 1$. Suppose, furthermore, that $\hat{x}[l]$ denotes the spectral measurements from underlying r Diracs. Then, we have*

$$\text{RANK} \mathcal{H}(\hat{\mathbf{x}}) = r. \quad (40)$$

Proof. Because $d \geq r + 1$, $n - d + 1 \geq r + 1$ and $\hat{x}[l]$ comes from (17), the associated Hankel matrix $\mathcal{H}(\hat{\mathbf{x}})$ has the decomposition structure as in (20). Furthermore, L and R are Vandermonde matrices that are full column-ranked. Hence,

$$\text{RANK} \mathcal{H}(\hat{\mathbf{x}}) = \text{RANK}(D) = r.$$

This concludes the proof. \square

Note that the construction of Hankel matrix in (19) by EMaC and in (36) by FRI sampling theory are identical if $\hat{x}[l]$ comes from the underlying r Diracs. However, it is important to note that Hankel matrix in (36) can be constructed for more general classes of FRI signals, and in this case the resulting Hankel matrix does not have decomposition structure (20). However, Proposition II.4 still informs that even in this case the Hankel structured matrix is still low-ranked. This is the main clue we exploit in this paper.

III. COMPRESSIVE SAMPLING OF FRI SIGNALS USING LOW-RANK INTERPOLATION

A. Stream of Differentiated Diracs

Another important class of FRI signal is a stream of differentiated Diracs given by

$$x(t) = \sum_{l \in \mathbb{Z}} \sum_{j=0}^{d_j} c_{lj} \delta^{(j)}(t - t_l) , \quad (41)$$

with the usual periodicity conditions $t_{l+r} = t_l + \tau$ and $c_{l+r,j} = c_{l,j}, \forall l \in \mathbb{Z}$, where $\delta^{(j)}$ denotes the j -th derivative of Diracs in the distributions sense. Because there exist $\tilde{r} = \sum_{j=0}^{r-1} d_j$ weights with unknown r locations, the rate of innovation is given by [11]–[13]:

$$\rho = \frac{r + \tilde{r}}{\tau} . \quad (42)$$

It was shown that the corresponding annihilating filter is [11]:

$$\hat{h}(z) = \prod_{j=0}^{r-1} (1 - u_j z^{-1})^{d_j} \quad (43)$$

where $u_j = e^{-i2\pi t_j/\tau}$ and Theorem II.1 hold with the minimum sampling rate

$$m \geq r + \tilde{r} + 1 . \quad (44)$$

For the case of stream of differentiated Diracs, the spectral measurement is

$$\hat{x}(\omega) = \sum_{l=0}^{r-1} \sum_{j=0}^{d_j} c_{lj} (i\omega)^j e^{-i\omega t_j} \quad (45)$$

and its discrete measurements can be represented by

$$\hat{x}[l] := \hat{x}(l\Delta) = \sum_{l=0}^{r-1} \sum_{j=0}^{d_j} c_{lj} \left(\frac{i2\pi l}{\tau} \right)^j e^{-i2\pi l t_j/\tau}, \quad m \in \Omega \quad (46)$$

which does not have the decomposition structure in (20). Therefore, this signal cannot be analyzed by the spectral compressed sensing by Chen and Chi [18]. On the other hand, the proposed low-rank interpolation framework using annihilating filter-based Hankel matrix can be still used to recovery signals. More specifically, from the z-transform in (43), the minimum length discrete annihilating filter $\hat{h}[n]$ has the length of $\tilde{r} + 1$. Therefore, for any k_1 tap size

filter $\hat{a}[n]$, the augmented filter $\hat{h}[n] = \hat{a}[n] * \hat{h}[n]$ is also an annihilating filter with $\kappa = \tilde{r} + k_1$ tap size. Accordingly, using the identical argument used for proving Proposition II.4, we can show the following as a simple corollary:

Corollary III.6. *For a given stream of differentiated Diracs in Eq. (41), let $\tilde{r} = \sum_{j=0}^{r-1} d_j$. Suppose, furthermore, d is given by $d \geq 1 + \tilde{r}$. Then, for a given Hankel structured matrix $\mathcal{H}(\hat{\mathbf{x}}) \in \mathcal{H}(n, d)$, we have*

$$\text{RANK} \mathcal{H}(\hat{\mathbf{x}}) \leq \tilde{r}. \quad (47)$$

Therefore, if some of the spectral measurement in $\hat{\mathbf{x}}$ are missing, we can use the structured low rank matrix completion frameworks in (24) to estimate $\hat{\mathbf{x}}$.

B. Non-uniform Splines

Note that signals may not be sparse in the image domain, but can be sparsified in a transform domain. Our goal is to find a generalized framework, whose sampling rate can be reduced down to the transform domain sparsity level. Specifically, the signal x of our interest is a non-uniform spline that can be represented by :

$$\mathbf{L}x = w \quad (48)$$

where \mathbf{L} denotes a constant coefficient linear differential equation (or whitening operator in [27], [28]):

$$\mathbf{L} := a_K \partial^K + a_{K-1} \partial^{K-1} + \dots + a_1 \partial + a_0 \quad (49)$$

and

$$w(t) = \sum_{j=0}^{r-1} c_j \delta(t - t_j) \quad . \quad (50)$$

For example, if the underlying signal is piecewise constant, we can set \mathbf{L} as the first differentiation. In this case, x corresponds to the total variation signal model.

Then, by taking the Fourier transform of (48), we have

$$\hat{y}(\omega) := \hat{l}(\omega) \hat{x}(\omega) = \sum_{j=0}^{r-1} a_j e^{-i\omega x_j} \quad (51)$$

where

$$\hat{l}(\omega) = a_K (i\omega)^K + a_{K-1} (i\omega)^{K-1} + \dots + a_1 (i\omega) + a_0 \quad (52)$$

Accordingly, the same filter $\hat{h}[n]$ that annihilates (46) can annihilate the weighted signal $\hat{l}(\omega) \hat{x}(\omega)$. Since the right hand side of (51) is same as (16), we can easily obtain the following results from Corollary II.5:

Corollary III.7. *Suppose that a non-uniform spline $x(t)$ is given by Eq. (48). Suppose, furthermore, d is given by $d \geq r + 1$ and $n - d + 1 \geq r + 1$. Then, for a given Hankel structured matrix $\mathcal{H}(\hat{\mathbf{y}}) \in \mathcal{H}(n, d)$ that is constructed*

using a discrete samples of $\hat{y}(\omega)$ in (51), we have

$$\text{RANK } \mathcal{H}(\hat{\mathbf{y}}) = r. \quad (53)$$

Thanks to the low-rankness, the missing spectral elements can be recovered using the following matrix completion problem:

$$\begin{aligned} (P_w) \quad & \min_{\mathbf{m} \in \mathbb{C}^n} \quad \|\mathcal{H}(\mathbf{m})\|_* \\ & \text{subject to} \quad P_\Omega(\mathbf{m}) = P_\Omega(\hat{\mathbf{l}} \odot \hat{\mathbf{x}}), \end{aligned} \quad (54)$$

where \odot denotes the Hadamard product, and $\hat{\mathbf{l}}$ and $\hat{\mathbf{x}}$ denotes the vectors composed of discrete samples of $\hat{l}(\omega)$ and $\hat{x}(\omega)$, respectively. Note that by solving (P_w) we can obtain the missing data $m(\omega) = \hat{l}(\omega)\hat{x}(\omega)$ in the Fourier domain. Then, the missing spectral data $\hat{x}(\omega)$ can be obtained by dividing by the weight, i.e. $\hat{x}(\omega) = m(\omega)/\hat{l}(\omega)$, when $\hat{l}(\omega) \neq 0$. As for the signal $\hat{x}(\omega)$ at the spectral null of the filter $\hat{l}(\omega)$, the corresponding elements should be included as sampled measurements.

C. Piecewise Polynomials

A signal is a periodic piecewise polynomial with r pieces each of maximum degree q if and only if its $(q+1)$ derivative is a stream of differentiated Diracs, that is, given by

$$x^{(q+1)}(t) = \sum_{l \in \mathbb{Z}} \sum_{j=0}^q c_{lj} \delta^{(j)}(t - t_l), \quad (55)$$

with the usual periodicity conditions. The degree of the freedom per period are r from the locations and $r(q+1)$ from the weighting coefficients, resulting in:

$$\rho = \frac{(q+2)r}{\tau}. \quad (56)$$

In this case, the corresponding Fourier transform relationship is given by

$$\hat{y}(\omega) := (i\omega)^{(q+1)} \hat{x}(\omega) = \sum_{l=0}^{r-1} \sum_{j=0}^q c_{lj} (i\omega)^j e^{-i\omega x_l}. \quad (57)$$

Since the righthand side of (57) is a special case of (45), the corresponding minimum length annihilating filter has the following z-transform representation:

$$\hat{h}(z) = \prod_{j=0}^{r-1} (1 - u_j z^{-1})^q. \quad (58)$$

From (58), the minimum annihilating filter filter size is $qr + 1$, and Theorem II.1 holds with the minimum FRI sampling rate given by

$$m \geq (q+1)r + 1.$$

Thus, using the identical argument for Proposition II.4, we can easily show that the Hankel structured matrix

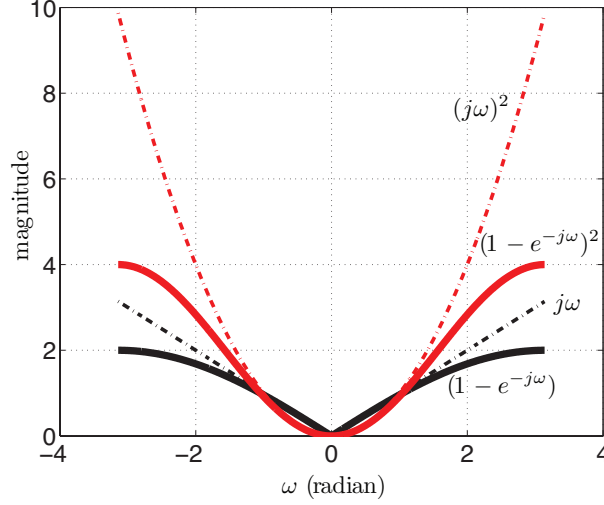


Fig. 2. Comparison of first- and second-order weights from whitening operator L and discrete counter-part L_d .

constructed by the discrete samples of $\hat{y}(\omega)$ in (57) is low-ranked.

Corollary III.8. *Suppose that a piecewise polynomial $x(t)$ has the $(q+1)$ -th derivative given by Eq. (55). Suppose, furthermore, d is given by $d \geq qr+1$. Then, for a given Hankel structured matrix $\mathcal{H}(\hat{\mathbf{y}}) \in \mathcal{H}(n, d)$ that is constructed using a discrete samples of $\hat{y}(\omega)$ in (57), we have*

$$\text{RANK} \mathcal{H}(\hat{\mathbf{y}}) \leq qr. \quad (59)$$

Similar to the non-uniform spline case, if some of the spectral measurements are missing, we can solve (P_w) with $\hat{l}(\omega) = (i\omega)^{(q+1)}$ to estimate the missing spectral components, from which the underlying piecewise polynomial signal can be estimated.

D. Cardinal Splines

One of the limitations of the proposed low-rank interpolation approach for the recovery of non-uniform splines and piecewise polynomials is that the weighting factor $\hat{l}(\omega)$ used in (P_w) is basically a high pass filter that can boost up the noise contribution. In particular, as shown in Fig. 2, $\hat{l}(\omega) = j\omega$ or $(j\omega)^2$ for the case of TV signals or the second order splines, respectively, where the high frequency components are more weighted. In particular, the noise boosting artifact becomes much severe for high order splines or polynomials. This may limit the performance of the overall low-rank matrix completion algorithm. Therefore, we need to devise a regularization scheme to limit the noise amplification.

In fact, another important advantage of the proposed low-rank interpolation approach is that it provides a natural regularization scheme by restricting the signal classes. More specifically, rather than attempting to recover FRI signals with arbitrary precision, if we recover signals that have cardinal spline representation, we can obtain a

regularized weighting factor for (P_w) that can limit the noise boosting. Therefore, this section is dedicated to discuss this important discovery.

The analysis in this section is significantly influenced by the theory of sparse stochastic processes [27], [28], [32], so we follow the original authors's notation. A cardinal spline is a special case of a general non-uniform spline where the knots are located on the integer grid [27], [28], [32]. More specifically, a function $x(t)$ is called a *cardinal L-spline* if and only if

$$Lx(t) = w(t), \quad (60)$$

where the operator L is same as in (49), and the continuous domain *innovation* signal $w(t)$ is given by

$$w(t) := \sum_{l \in \mathbb{Z}} a[l] \delta(t - l), \quad (61)$$

whose singularities are located on integer grid. For this cardinal splines, we are now interested in deriving the discrete counterpart of the whitening operator L , which is denoted by L_d . The corresponding continuous domain description of its impulse response is

$$L_d \delta(t) = \sum_{l \in \mathbb{Z}} d_L[l] \delta(t - l).$$

The main advantage of using L_d is that we can recover signals by exploiting the sparseness of *discrete innovation* rather than exploiting off-grid singularity. Specifically, define a generalized B-spline associated with the operator L [32]

$$\beta_L(t) = L_d L^{-1} \delta(t) = \mathcal{F}^{-1} \left\{ \frac{\sum_{l \in \mathbb{Z}} d_L[l] e^{-j\omega l}}{\hat{l}(\omega)} \right\} (t), \quad (62)$$

which provides the equivalent B-spline representation of $x(t)$ in (60):

$$x(t) = \sum_{l \in \mathbb{Z}} c[l] \beta_L(t - l). \quad (63)$$

The equivalence can be easily shown by

$$Lx(t) = \sum_{l \in \mathbb{Z}} c[l] L \beta_L(t - l) = \sum_{l \in \mathbb{Z}} \underbrace{(c * d_L)[l]}_{a[l]} \delta(t - l), \quad (64)$$

because $LL_d L^{-1} \delta(t) = L_d \delta(t)$. Now, by applying the discrete version of whitening operator L_d , we have

$$\begin{aligned} u_c(t) &:= L_d x(t) = L_d L^{-1} w(t) = (\beta_L * w)(t) \\ &= \sum_{l \in \mathbb{Z}} a[l] \beta_L(t - l). \end{aligned} \quad (65)$$

As shown in Fig. 3, this is indeed a *smoothed* version of continuous domain innovation $w(t)$ in (61), because all the sparsity information of the innovation $w(t)$ is encoded in its coefficients $\{a[l]\}$; and, aside from the interpolant $\beta_L(t)$, $u_c(t)$ in (65) still retains the same coefficients. Moreover, the sampled discrete innovation on the integer

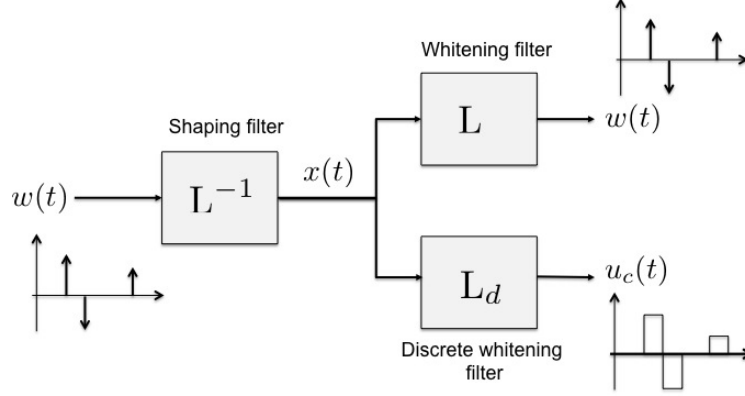


Fig. 3. The discrete innovation and continuous domain innovations generated by L_d and L , respectively.

grid can be obtained from the following impulse sampling of $u_c(t)$:

$$\begin{aligned} u(t) &:= u_c(t) \sum_{l \in \mathbb{Z}} \delta(t - l) \\ &= \sum_{l \in \mathbb{Z}} u[l] \delta(t - l) \end{aligned} \quad (66)$$

$$= \sum_{l \in \mathbb{Z}} (a * b_L)[l] \delta(t - l) \quad (67)$$

$$= \sum_{l \in \mathbb{Z}} (d_L * c * b_L)[l] \delta(t - l) \quad (68)$$

$$= \sum_{l \in \mathbb{Z}} (d_L * x_L)[l] \delta(t - l) \quad (69)$$

where we use $a[l] = (d_L * c)[l]$ and

$$b_L[l] := \beta_L(t)|_{t=l}, \quad (70)$$

and

$$x_L[k] := x(t)|_{t=k} = \sum_{l \in \mathbb{Z}} c[l] \beta(k - l) = (c * b_L)[k]. \quad (71)$$

This result informs us several ways to make the *discrete innovation* $u[l]$ sparse. First, if $a[l]$ in (60) is sparse, then the discrete filter $b_L[k]$ should be designed to have the minimum size. Due to the relationship (70), this can be achieved if $\beta_L(t)$ is maximally localized. Second, if the property of discrete sample $x[l]$ is known, then we can design a discrete innovation filter $d_L[l]$ such that the filtered signal $(d_L * x_L)[l]$ is maximally sparse. This sparseness of the discrete innovation is the property we exploit in recovering the missing spectral measurements.

Specifically, let $\{u_j\}_{j=0}^{r-1}$ denotes the set of nonzero coefficients of $\{u[l]\}$ such that $u_j = u[l_j]$ with l_j as the corresponding index. We further define n such that for all $\{l_j\}_{j=0}^{r-1} \subset [0, \dots, n-1]$. Then, the corresponding

discrete spectrum with the sampling interval $2\pi/n$ is given by

$$\hat{u}[k] = \hat{u}(\omega)|_{\omega=\frac{2\pi k}{n}} = \sum_{j=0}^{r-1} u_j e^{-i\frac{2\pi k l_j}{n}}$$

which corresponds to the DFT of the discrete innovation $u[l]$. Then, the minimum size annihilating filter $\hat{h}[k]$ with respect to $\hat{u}[k]$ can be obtained from the following z-transform expression

$$\hat{h}(z) = \prod_{j=0}^{r-1} (1 - e^{-i\frac{2\pi k l_j}{n}} z^{-1}) \quad (72)$$

Thanks to the sparseness of the discrete innovation, the following corollary can be easily obtained:

Corollary III.9. *Suppose that a function $x(t)$ is a cardinal L-spline given by (60). Suppose, furthermore, its discrete innovation $u[n]$ defined by (65) and (66) is r -sparse. Then, for the given DFT spectrum*

$$\hat{u}[k] = \hat{d}_L(\omega) \hat{x}_L(\omega) \Big|_{\omega=\frac{2\pi k}{n}} = \hat{d}_L[k] \hat{x}_L[k], \quad k = 0, \dots, n-1$$

and the associated Hankel structured matrix $\mathcal{H}(\hat{\mathbf{u}}) \in \mathcal{H}(n, d)$ such that $d \geq r + 1$, we have

$$\text{RANK} \mathcal{H}(\hat{\mathbf{u}}) \leq r. \quad (73)$$

Note that we can easily estimate the sparsity r of the discrete innovation. Specifically, if the number of underlying Diracs is s (i.e. the number of nonzero $a[l]$ is s) and the length of $b_L[k]$ is n_b , then the sparsity level of the discrete innovation is upper bounded by

$$r \leq n_b s. \quad (74)$$

Therefore, if the resulting sparsity is sufficiently small, we can exploit the low-rankness of $\mathcal{H}(\hat{\mathbf{u}})$ and solve (P_w) to estimate the missing spectral components.

However, compared to the previous analysis, there exist additional important distinctions. First, due to the uniform sampling of the discrete innovation, the corresponding $\hat{u}[k]$ is also periodic with the period of n . Thanks to the periodicity of $\hat{u}[k]$, we can use the following circulant matrix:

$$\mathcal{H}_c(\hat{\mathbf{u}}) = \begin{bmatrix} \hat{u}[0] & \hat{u}[1] & \cdots & \hat{u}[d-1] \\ \hat{u}[1] & \hat{u}[2] & \cdots & \hat{u}[d] \\ \vdots & \vdots & \ddots & \vdots \\ \hat{u}[n-d] & \hat{u}[n-d+1] & \cdots & \hat{u}[n-1] \\ \hline \hat{u}[n-d+1] & \hat{u}[n-d+2] & \cdots & \hat{u}[0] \\ \vdots & \vdots & \ddots & \vdots \\ \hat{u}[n-1] & \hat{u}[0] & \cdots & \hat{u}[d-2] \end{bmatrix} \in \mathbb{C}^{n \times d} \quad (75)$$

where the bottom block is augmented block compared to the original Hankel matrix construction (19). Since the

bottom block can be also annihilated using the same annihilating filter, we can see the rank of the circulant expansion is the same as the original Hankel structured matrix:

$$\text{RANK } \mathcal{H}_c(\hat{\mathbf{u}}) = \text{RANK } \mathcal{H}(\hat{\mathbf{u}}).$$

The main advantage of (75) is that every elements of spectral measurement $\hat{u}[k], k = 0, \dots, n-1$ has uniform d contribution, compared to (19) in which some elements has only a single contribution. This makes the estimation of spectral vector $\hat{\mathbf{u}}$ more reliable. Second, in constructing the weighting matrix $\hat{l}(\omega)$ for the low-rank matrix completion problem (P_w), instead of using spectrum of the original whitening operator L , we should use $\hat{l}_d(\omega)$ which is the Fourier transform of the discrete counterpart L_d . As will be shown in the following examples, this helps to limit the noise amplification in the associated low-rank matrix completion problem.

1) *Signals with Total Variation*: A signal with total variation can be considered as a special case of (60) with $L = \frac{d}{dt}$. Then, the discrete whitening operator L_d is the finite difference operator D_d given by

$$D_d x(t) = x(t) - x(t-1).$$

In this case, the associated L -spline is given by

$$\beta_L(t) = \beta_+^0(t) = \mathcal{F}^{-1} \left\{ \frac{1 - e^{-j\omega}}{j\omega} \right\} (t) = \begin{cases} 1, & \text{for } 0 \leq t < 1 \\ 0, & \text{otherwise} \end{cases} \quad (76)$$

Note that this is maximally localized spline because $b_L[k] = \beta_L(t)|_{t=k} = \delta[k]$ is a single tab filter (i.e. $n_b = 1$). Therefore, according to (74), the sparsity level of the discrete innovation is equal to the number of underlying Diracs. Moreover, the weighting function for the low-rank matrix completion problem in (P_w) is given by

$$\hat{l}_d(\omega) = 1 - e^{-j\omega}.$$

Figure 2 compared the weighting functions that corresponds to the original whitening operator $\hat{l}(\omega) = j\omega$ and the discrete counterpart $\hat{l}_d(\omega) = 1 - e^{-j\omega}$. We can clearly see that high frequency boosting is reduced by the discrete whitening operator, which makes the low-rank matrix completion much more robust.

2) *Signals with Higher order Total Variation*: Consider a signal $x(t)$ that is represented by (60) with $L = \frac{d^{m+1}}{dt^{m+1}}$. Then, the corresponding discrete counterpart L_d should be constructed by

$$L_d \delta(t) = \underbrace{D_d D_d \cdots D_d}_m \delta(t).$$

In this case, the associated L -spline is given by [32]

$$\begin{aligned} \beta_+^m(t) &= \underbrace{(\beta_+^0 * \beta_+^0 * \cdots * \beta_+^0)}_{m+1}(t) \\ &= \mathcal{F}^{-1} \left\{ \left(\frac{1 - e^{-j\omega}}{j\omega} \right)^{m+1} \right\} (t) = \sum_{k=0}^{m+1} (-1)^k \binom{m+1}{k} \frac{(t-k)_+^m}{m!} \end{aligned} \quad (77)$$

with $(t)_+ = \max(0, t)$. We can see that the length of the corresponding filter $b_L[n]$ is now given by $n_b = m + 1$. Hence, when the underlying signal is s -Diracs, then the sparsity level of the discrete innovation is upper bounded by

$$r \leq (m + 1)s, \quad (78)$$

and the corresponding weighting function for (P_w) is given by

$$\hat{l}_d(\omega) = (1 - e^{-j\omega})^{m+1}. \quad (79)$$

Again, Figure 2 clearly showed that this weighting function is much more noise robust compared to the original weighting $(j\omega)^{m+1}$.

In general, the relationship between the sparsity and the noise reduction by (78) and (79) clearly demonstrated the trade-off between regularization and the resolution in signal recovery. Specifically, to recover high order splines, rather than imposing the higher order weighting that is prone to noise boosting, we can use regularised weighting (79) that comes from discrete whitening operator. The catch, though, is the necessity for additional spectral samples originated from the sparsity increase in (78).

IV. FUNDAMENTAL SAMPLING PERFORMANCE

So far, we have provided a generalization to deal with a variety of signals. The main goal of this section is to derive the fundamental sampling performance, which is another contribution of this paper. In fact, we will show that such generalisation do not lose the optimality compared to the standard compressed sensing approaches.

Toward this goal, we first investigate the properties of bases that generate spaces of structured matrices.

A. Basis of Structured Matrices

A Hankel structured matrix in $\mathcal{H}(n, d)$ can be represented using the basis

$$B_k = \begin{cases} \frac{1}{\sqrt{k}} \sum_{i=1}^k \mathbf{e}_i \mathbf{e}_{k-i+1}^*, & k = 1, \dots, d \\ \frac{1}{\sqrt{d}} \sum_{i=1}^d \mathbf{e}_i \mathbf{e}_{k-i+1}^*, & k = d + 1, \dots, n - d + 1 \\ \frac{1}{\sqrt{n-k+1}} \sum_{i=k-n+d}^d \mathbf{e}_i \mathbf{e}_{k-i+1}^*, & k = n - d + 2, \dots, n \end{cases} \quad (80)$$

Similarly, a circulant matrix in $\mathcal{H}_c(n, d)$ has the following basis

$$B_k = \frac{1}{\sqrt{d}} \sum_{i=1}^d \mathbf{e}_i \mathbf{e}_{[k-i]_{(n)}+1}^*, \quad k = 1, \dots, n. \quad (81)$$

where $[\cdot]_n$ denotes the modulo operation that finds the remainder after division by n .

These basis for structured matrix is composed of linear sums of standard matrix basis $\{\mathbf{e}_i \mathbf{e}_j^*\}_{i,j=1}^{d,n-d+1}$. We can further show

$$\langle \mathbf{e}_{i_1} \mathbf{e}_{j_1}^*, \mathbf{e}_{i_2} \mathbf{e}_{j_2}^* \rangle = \text{Tr}(\mathbf{e}_{j_1} \mathbf{e}_{i_1}^* \mathbf{e}_{i_2} \mathbf{e}_{j_2}^*) = \delta_{i_1, i_2} \text{Tr}(\mathbf{e}_{j_1} \mathbf{e}_{j_2}^*) = \delta_{i_1, i_2} \delta_{j_1, j_2} \quad (82)$$

because there exist no non-zero diagonal components unless $j_1 = j_2$. Using this property, we can now derive the following properties of basis for structured matrices.

Lemma IV.10. *Let $\{B_k\}_{k=1}^n$ denote the basis of a space of Hankel matrix $\mathcal{H}(n, d)$. Then, for all i, j, k , we have*

$$\|B_k\| \leq 1, \quad \|B_k\|_F^2 = 1, \quad \langle B_i, B_j \rangle = \delta_{i,j} \quad (83)$$

Proof. First, consider $n - d + 1 > d$. Define a vector $\chi_{p:q}^n$ such that

$$\chi_{p:q}^n = \begin{bmatrix} \underbrace{0 \cdots 0}_{p-1} & \underbrace{1 \cdots 1}_{q-p+1} & \underbrace{0 \cdots 0}_{n-q} \end{bmatrix}$$

Then, a simple application of (82) provides us

$$B_k^* B_k = \begin{cases} \frac{1}{k} \text{Diag}(\chi_{1:k}^d), & k \leq d \\ \frac{1}{d} \text{Diag}(\chi_{1:d}^d), & d+1 \leq k \leq n-d+1 \\ \frac{1}{n-k+1} \text{Diag}(\chi_{k-n+d:d}^d), & n-d+2 \leq k \leq n \end{cases} \quad (84)$$

$$B_k B_k^* = \begin{cases} \frac{1}{k} \text{Diag}(\chi_{1:k}^{n-d+1}), & k \leq d \\ \frac{1}{d} \text{Diag}(\chi_{k-d+1:k}^{n-d+1}), & d+1 \leq k \leq n-d+1 \\ \frac{1}{n-k+1} \text{Diag}(\chi_{k-d+1:n-d+1}^{n-d+1}), & n-d+2 \leq k \leq n \end{cases} \quad (85)$$

where $\text{Diag}(\cdot)$ denotes a diagonalization operator from a vector. Since $B_k^* B_k$ is a diagonal matrix for each k , $\|B_k\|^2$ is equal to the maximum value of diagonal entries of $B_k^* B_k$ so that $\|B_k\| \leq 1$ for each k . Next, according to (82), to have non-zero inner product, there should exist at least one common standard matrix basis between two Hankel basis. However, due to the non-overlapping structure of Hankel basis, there is no common matrix basis; so we can easily see that $\langle B_i, B_j \rangle = 0$ when $i \neq j$. Furthermore, $\langle B_i, B_i \rangle = \|B_i\|_F^2 = 1$. This concludes the proof. \square

For the cases of circulant matrices, the algebra is much simpler.

Corollary IV.11. *Let $\{B_k\}_{k=1}^n$ denote the basis of a space of circulant matrix $\mathcal{H}_c(n, d)$. Then, for all i, j, k , we have*

$$\|B_k\| = 1, \quad \|B_k\|_F^2 = 1, \quad \langle B_i, B_j \rangle = \delta_{i,j} \quad (86)$$

Proof. Then, a simple application of (82) provides us

$$B_k^* B_k = \frac{1}{d} I_d, \quad B_k B_k^* = \begin{cases} \frac{1}{d} \text{Diag}(\chi_{k-d+1:k}^n), & \text{if } k \geq d \\ \frac{1}{d} (\text{Diag}(\chi_{1:k}^n) + \text{Diag}(\chi_{n-d+k+1:d-k}^n)), & \text{if } 1 \leq k < d \end{cases} \quad (87)$$

where I_d denotes the $d \times d$ identity matrix. Accordingly, we have $\|B_k\| = 1, \|B_k\|_F^2 = 1$. The remainder of the proof is identical to those of Lemma IV.10. \square

Lemma IV.12. 1) Let $\{B_k\}_{k=1}^n$ denote the basis of a space of Hankel matrix $\mathcal{H}(n, d)$. Then, for $n - d + 1 \geq d$,

$$\begin{aligned} \max\{\|\sum_{k=1}^n B_k^* B_k\|, \|\sum_{k=1}^n B_k B_k^*\|\} &= \frac{n - 2d + 1}{d} + \sum_{k=1}^d \frac{1}{k} \\ &\leq \frac{n - d + 1}{d} + \log(d) := \alpha(n, d) \end{aligned} \quad (88)$$

where we use $\sum_{k=1}^n \frac{1}{k} \leq 1 + \log(n)$. Otherwise, we have

$$\begin{aligned} \max\{\|\sum_{k=1}^n B_k^* B_k\|, \|\sum_{k=1}^n B_k B_k^*\|\} &= \frac{n - 2d + 1}{n - d + 1} + \sum_{k=1}^{n-d+1} \frac{1}{k} \\ &\leq 2 - \frac{d}{n - d + 1} + \log(n - d + 1) := \alpha(n, d) \end{aligned} \quad (89)$$

2) Let $\{B_k\}_{k=1}^n$ denote the basis of a space of circulant matrix $\mathcal{H}_c(n, d)$ with $n \geq d$. Then,

$$\alpha(n, d) := \max\{\|\sum_{k=1}^n B_k^* B_k\|, \|\sum_{k=1}^n B_k B_k^*\|\} = \frac{n}{d}. \quad (90)$$

Proof. We start with the Hankel matrix cases. First, consider the case $(n - d + 1) \geq d$. We split the summation into the following three sum:

$$\sum_{k=1}^n B_k^* B_k = \sum_{k=1}^d B_k^* B_k + \sum_{k=d+1}^{n-d+1} B_k^* B_k + \sum_{k=n-d+2}^n B_k^* B_k$$

Owing to (84), we know that the i -th diagonal element of $\sum_{k=1}^n B_k^* B_k$ is given by the following identity :

$$\sum_{k=i}^d \frac{1}{k} + \sum_{k=d+1}^{n-d+1} \frac{1}{d} + \sum_{k=n-d+2}^{n-d+i} \frac{1}{n-k+1} \leq \sum_{k=1}^d \frac{1}{k} + \sum_{k=d+1}^{n-d+1} \frac{1}{d}$$

where the RHS is equal to the first diagonal element (i.e. $i = 1$) of $\sum_{k=1}^n B_k^* B_k$, and the inequality comes from

$$\sum_{k=n-d+2}^{n-d+i} \frac{1}{n-k+1} = \sum_{l=1}^{i-1} \frac{1}{d-l} = \sum_{p=1}^{i-1} \frac{1}{d-i+p} \leq \sum_{p=1}^{i-1} \frac{1}{p}.$$

Therefore, $\|\sum_{k=1}^n B_k^* B_k\| = \alpha(n, d)$. Similarly, we can find that the i -th entry of $\sum_{k=1}^n B_k B_k^*$ is given by $\sum_{k=1}^d \frac{1}{k}$, so that we have the desired result. The case $d > n - d + 1$ can be similarly handled.

For the case of circulant matrix, the proof is straightforward due to (87). \square

B. Sampling Condition for Structured Matrix Completion

Define a corresponding sampling operator to the k -th coefficient:

$$R_k(M) = \langle B_k, M \rangle B_k, \quad k = 1, \dots, n$$

where $\{B_k\}_{k=1}^n$ is an orthonormal basis of $\mathcal{H}(n, d)$ (or $\mathcal{H}_c(n, d)$) such that

$$\langle B_k, B_j \rangle = \delta_{i,j}.$$

Then, for a given sampling index set Ω , the sampled measurement of the matrix is given by

$$R_\Omega(M) = \sum_{k \in \Omega} \langle B_k, M \rangle B_k.$$

We can derive the expansion coefficients energy.

Lemma IV.13. *For a structured matrix M in $\mathcal{H}(n, d)$ or $\mathcal{H}_c(n, d)$, suppose that we have $M = \sum_{k=1}^n \langle B_k, M \rangle B_k$. Then, the following identity holds:*

$$\sum_{k=1}^n \langle B_k, M \rangle^2 = \|M\|_F^2 \quad (91)$$

Proof. Note that

$$\begin{aligned} \|M\|_F^2 = \langle M, M \rangle &= \sum_{k=1}^n \sum_{l=1}^n \langle B_k, M \rangle^* \langle B_l, M \rangle \langle B_k, B_l \rangle \\ &= \sum_{k=1}^n \langle B_k, M \rangle^2 \|B_k\|_F^2 \\ &= \sum_{k=1}^n \langle B_k, M \rangle^2 \end{aligned}$$

where we use the last properties in (83) and (86) for the second equality, and the last inequality trivially follows from $\|B_k\|_F^2 = 1$ for all k . This concludes the proof. \square

Now, for a given structured matrix M in $\mathcal{H}(n, d)$ or $\mathcal{H}_c(n, d)$ with sampling index set Ω , our problem is to find the sampling condition for the following structured matrix completion problem. We first consider the noiseless recovery problem:

$$\begin{aligned} (P) \quad & \min \|X\|_* \\ \text{subject to} \quad & R_\Omega(X) = R_\Omega(M). \end{aligned}$$

Note that the structured matrix M is constructed from n -dimensional vector and many of the matrix elements are thus sampled simultaneous, so the degree of freedom in matrix is limited by n . Therefore, we denote the sampling index $\Omega \subset [0, \dots, n-1]$.

Suppose that M is a structured matrix of rank r with the singular value decomposition $U\Sigma V^*$ with $U = [\mathbf{u}_1, \dots, \mathbf{u}_r]$ and $V = [\mathbf{v}_1, \dots, \mathbf{v}_r]$. Let T be the linear space spanned by elements of the form $\mathbf{u}_k \mathbf{y}^*$ and $\mathbf{x} \mathbf{v}_k^*$, $1 \leq k \leq r$, where \mathbf{x} and \mathbf{y} are arbitrary, and T^\perp is its orthogonal complement. Then, the orthogonal projection P_T onto T is given by

$$P_T(Z) = P_U Z + Z P_V - P_U Z P_V \quad (92)$$

where P_U and P_V are the orthogonal projection onto U and V , respectively. We now define the following:

Definition IV.1. 1) Suppose that $M \in \mathcal{H}(n, d)$ is an $(n - d + 1) \times d$ matrix of rank r with the singular value decomposition $U\Sigma V^*$. Then, the coherence of U in relation to the basis $\{B_k\}$ is defined to be

$$\mu_0 = \max_k \left\{ \frac{n - d + 1}{r} |\langle B_k, P_U B_k \rangle|, \frac{d}{r} |\langle B_k, B_k P_V \rangle| \right\} \quad (93)$$

$$\mu_1 = \frac{\max(d, n - d + 1)}{r} \|UV^*\|_\infty. \quad (94)$$

2) Suppose that $M \in \mathcal{H}_c(n, d)$ is an $n \times d$ circulant matrix of rank r with the singular value decomposition $U\Sigma V^*$. Then, the coherence of U in relation to the basis $\{B_k\}$ is defined to be

$$\mu_0 = \max_k \left\{ \frac{n}{r} |\langle B_k, P_U B_k \rangle|, \frac{d}{r} |\langle B_k, B_k P_V \rangle| \right\} \quad (95)$$

$$\mu_1 = \frac{n}{r} \|UV^*\|_\infty. \quad (96)$$

From (92), we have

$$P_T(B_k) = P_U B_k + B_k P_V - P_U B_k P_V$$

Using Eqs. (93) and (94) (resp. Eqs. (95) and (96)), this gives us

$$|\langle B_k, P_T(B_k) \rangle| \leq |\langle B_k, P_U B_k \rangle| + |\langle B_k, B_k P_V \rangle| \leq \frac{2\mu_0 r}{n} c_s \quad (97)$$

where

$$c_s = \begin{cases} \max \left\{ \frac{n}{d}, \frac{n}{n-d+1} \right\}, & M \in \mathcal{H}(n, d) \\ \frac{n}{d}, & M \in \mathcal{H}_c(n, d) \end{cases} \quad (98)$$

Then, by extending the work of Recht [33], we have the following result:

Theorem IV.14. Suppose that Ω is the set of entries of M that are observed with locations sampled uniformly at random from indices $[0, \dots, n - 1]$ and $m := |\Omega|$, and let $n \geq 3$. Then, if

$$m > 32\beta c_s \max\{\mu_0, \frac{3}{32}\gamma\mu_1\} r \log^2(2n) \quad (99)$$

where

$$\gamma = \frac{2}{3} \left(1 + \sqrt{1 + \frac{3}{2}\alpha(n, d)} \right) \quad (100)$$

and some $\beta > 1$ and $\alpha(n, d)$ is given by (88) or (89) (resp. (90) for circulant matrix), then the minimizer to problem (P) is unique and equal to M with probability at least $1 - \frac{3}{2} \log(n) n^{1-\beta} - n^{2-2\beta^{1/2}}$.

Proof. See Appendix A. □

In practice, measurements are often contaminated by a certain amount of noise. Our model for the noisy measurement M_0 is given by

$$R_\Omega(M_0) = R_\Omega(M) + R_\Omega(Z)$$

where $R_\Omega(Z)$ is a noise term. We assume that $\|R_\Omega(Z)\|_F \leq \delta$ for some $\delta > 0$. Then, to recover the unknown matrix, we solve the following optimization problem:

$$\begin{aligned} (P_{noisy}) \quad & \min \|X\|_* \\ \text{subject to} \quad & \|R_\Omega(X) - R_\Omega(M_0)\| \leq \delta. \end{aligned}$$

Following Candes and Plan [34], we can prove the following stability theorem:

Theorem IV.15. *Suppose $Y \in \mathcal{H}(n, d)$ is a noisy copy of $M \in \mathcal{H}(n, d)$ that satisfies $\|R_\Omega(X) - R_\Omega(Y)\| \leq \delta$. Under the condition for Theorem IV.14, the solution \hat{M} for P_{noisy} satisfies*

$$\|\hat{M} - M\|_F \leq 2\delta \left[1 + \left(1 + \frac{3}{2} \sqrt{rc_s \max \left\{ \mu_0, \frac{3}{32} \gamma \mu_1 \right\}} \right) \frac{2r}{1 - \sqrt{8/3}} \right] \quad (101)$$

at least $1 - \frac{3}{2} \log(n) n^{1-\beta} - n^{2-2\beta^{1/2}}$.

Proof. See Appendix B. □

V. ALGORITHM IMPLEMENTATION

A. Noiseless structured matrix completion algorithm

In order to solve structured matrix completion problem (P) using noise free measurements, we employ an SVD-free structured rank minimization algorithm [35] with an initialization using the low-rank factorization model (LMaFit) algorithm [36]. This algorithm does not use the singular value decomposition (SVD), so the computational complexity can be significantly reduced. Specifically, the algorithm is based on the following observation [37]:

$$\|A\|_* = \min_{U, V: A = UV^H} \|U\|_F^2 + \|V\|_F^2. \quad (102)$$

Hence, (24) can be reformulated as the nuclear norm minimization problem under the matrix factorization constraint:

$$\begin{aligned} \min_{U, V: \mathcal{H}(\mathbf{m}) = UV^H} \quad & \|U\|_F^2 + \|V\|_F^2 \\ \text{subject to} \quad & P_\Omega(\mathbf{m}) = P_\Omega(\hat{\mathbf{x}}), \end{aligned} \quad (103)$$

By combining the two constraints, we have the following cost function for an alternating direction method of multiplier (ADMM) step [38]:

$$\begin{aligned} L(U, V, \mathbf{m}, \Lambda) \quad & := \quad \iota(\mathbf{m}) + \frac{1}{2} (\|U\|_F^2 + \|V\|_F^2) \\ & \quad + \frac{\mu}{2} \|\mathcal{H}(\mathbf{m}) - UV^H + \Lambda\|_F^2 \end{aligned} \quad (104)$$

where $\iota(\mathbf{m})$ denotes an indicator function:

$$\iota(\mathbf{m}) = \begin{cases} 0, & \text{if } P_\Omega(\mathbf{m}) = P_\Omega(\hat{\mathbf{x}}) \\ \infty, & \text{otherwise} \end{cases}.$$

One of the advantages of the ADMM formulation is that each subproblem is simply obtained from (104). More specifically, $\mathbf{m}^{(n+1)}$, $U^{(n+1)}$ and $V^{(n+1)}$ can be obtained, respectively, by applying the following optimization problems sequentially:

$$\begin{aligned}\mathbf{m}^{(n+1)} &= \arg \min_{\mathbf{m}} \iota(\mathbf{m}) + \frac{\mu}{2} \|\mathcal{H}(\mathbf{m}) - U^{(n)} V^{(n)H} + \Lambda^{(n)}\|_F^2 \\ U^{(n+1)} &= \arg \min_U \frac{1}{2} \|U\|_F^2 + \frac{\mu}{2} \|\mathcal{H}(\mathbf{m}^{(n+1)}) - UV^{(n)H} + \Lambda^{(n)}\|_F^2 \\ V^{(n+1)} &= \arg \min_V \frac{1}{2} \|V\|_F^2 + \frac{\mu}{2} \|\mathcal{H}(\mathbf{m}^{(n+1)}) - U^{(n+1)} V^H + \Lambda^{(n)}\|_F^2\end{aligned}\quad (105)$$

and the Lagrangian update is given by

$$\Lambda^{(n+1)} = \mathcal{Y}^{(n+1)} - U^{(n+1)} V^{(n+1)H} + \Lambda^{(n)}.$$

It is easy to show that the first step in (105) can be reduced to

$$\mathbf{m}^{(n+1)} = P_{\Omega^c} \mathcal{H}^\dagger \left\{ U^{(n)} V^{(n)H} - \Lambda^{(n)} \right\} + P_{\Omega}(\hat{\mathbf{x}}), \quad (106)$$

where P_{Ω^c} is a projection mapping on the set Ω^c and \mathcal{H}^\dagger corresponds to the Penrose-Moore pseudo-inverse mapping from our structured matrix to a vector. Hence, the role of the pseudo-inverse is taking the average value and putting it back to the original coordinate. Next, the subproblem for U and V can be easily calculated by taking the derivative with respect to each matrix, and we have

$$\begin{aligned}U^{(n+1)} &= \mu (\mathcal{Y}^{(n+1)} + \Lambda^{(n)}) V^{(n)} (I + \mu V^{(n)H} V^{(n)})^{-1} \\ V^{(n+1)} &= \mu (\mathcal{Y}^{(n+1)} + \Lambda^{(n)})^H U^{(n+1)} (I + \mu U^{(n+1)H} U^{(n+1)})^{-1}\end{aligned}\quad (107)$$

Note that the computational complexity of our ADMM algorithm is dependent on the matrix inversion in (107), whose complexity is determined by the estimated rank of the structured matrix. Therefore, even though the structured matrix has large size, the estimated rank is much smaller, which significantly reduces overall complexity.

Now, for faster convergence, the remaining issue is how to initialize U and V . For this, we employ an algorithm called the low-rank factorization model (LMaFit) [36]. More specifically, for a low-rank matrix Z , LMaFit solves the following optimization problem:

$$\min_{U, V, Z} \frac{1}{2} \|UV^H - Z\|_F^2 \text{ subject to } P_I(Z) = P_I(\mathcal{H}(\hat{\mathbf{x}})) \quad (108)$$

and Z is initialized with $\mathcal{H}(\hat{\mathbf{x}})$ and the index set I denotes the positions where the elements of $\mathcal{H}(\hat{\mathbf{x}})$ are known. LMaFit solves a linear equation with respect to U and V to find their updates and relaxes the updates by taking the average between the previous iteration and the current iteration. Moreover, the rank estimation can be done automatically. LMaFit uses QR factorization instead of SVD, so it is also computationally efficient.

B. Noisy structured matrix completion algorithm

Similarly, the noisy matrix completion problem in (27) can be solved by minimizing the following Lagrangian function:

$$\begin{aligned} L(U, V, \mathbf{m}, \Lambda) &:= \frac{\lambda}{2} \|P_{\Omega}(\hat{\mathbf{y}}) - P_{\Omega}(\mathbf{m})\|_2^2 + \frac{1}{2} (\|U\|_F^2 + \|V\|_F^2) \\ &\quad + \frac{\mu}{2} \|\mathcal{H}(\mathbf{m}) - UV^H + \Lambda\|_F^2 \end{aligned} \quad (109)$$

where λ denotes an appropriate regularization parameter. Compared to the noiseless cases, the only difference is the update step of \mathbf{m} . More specifically, we have

$$\mathbf{m}^{(n+1)} = \arg \min_{\mathbf{m}} \frac{\lambda}{2} \|P_{\Omega}(\hat{\mathbf{y}}) - P_{\Omega}(\mathbf{m})\|_2^2 + \frac{\mu}{2} \|\mathcal{H}(\mathbf{m}) - U^{(n)}V^{(n)H} + \Lambda^{(n)}\|_F^2 \quad (110)$$

which can be reduced to

$$\mathbf{m}^{(n+1)} = P_{\Omega^c} \mathcal{H}^\dagger \left\{ U^{(n)}V^{(n)H} - \Lambda^{(n)} \right\} + P_{\Omega}(\mathbf{z}) \quad (111)$$

where $\mathbf{z} = [z[0], \dots, z[n-1]]^T$ such that

$$z[i] = \frac{\lambda y[i] + \mu P_i \left(\mathcal{H}^* \left(U^{(n)}V^{(n)H} - \Lambda^{(n)} \right) \right)}{\lambda + \mu P_i \left(\mathcal{H}^* \mathcal{H}(\mathbf{e}_i) \right)}, \quad (112)$$

where \mathbf{e}_i denotes the unit coordinate vector where the i -th element is 1, and P_i is the projection operator to the i -th coordinate.

VI. NUMERICAL RESULTS

The numerical comparison of the structured matrix completion for Diracs in off-grid has been extensively performed by Chen and Chi [18], so in this section, we mainly performed comparative study for recovering FRI signals on integer grid, because only in this scenario we can do the fair comparison with respect to the existing compressed sensing approach for discrete signals.

A. Noiseless Experiments

In this section, we perform numerical simulations to verify the proposed algorithm using noiseless measurements. Specifically, we consider three scenario: 1) streams of Diracs, 2) piecewise constant signals, and 3) super-position of Diracs and piecewise constant signals. Note that the last scenario is a special case of piecewise polynomial signals. As a reference for comparison, the basis pursuit (BP) algorithm [39] was used for recovering a stream of Diracs, whereas the split Bregman method of l_1 total variation reconstruction [40] was used for recovering signals in 2) and 3) scenario. For fair comparison, we assume that all the singularities are located on integer grid. To quantify recovery performances, phase transition plots were calculated using 300 Monte Carlo runs.

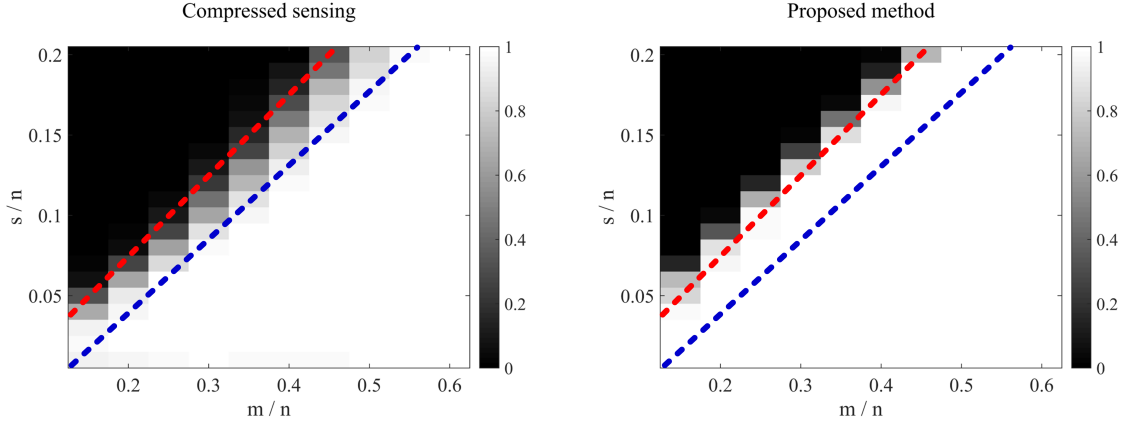


Fig. 4. Phase transition diagrams for recovering stream of Diracs from m random sampled Fourier samples. The size of target signal (n) is 100 and the annihilating filter size d was set to be 51. s denotes the number of Diracs. The left and right graphs correspond to the phase transition diagram of the basis pursuit [39] compressed sensing approach and the proposed low-rank interpolation approach, respectively. The success ratio is obtained by the success ratio from 300 Monte Carlo runs. Two transition lines from compressed sensing (blue) and low-rank interpolator (red) are overlaid.

1) *Diracs streams*: To simulate Diracs stream signals, we generated one-dimensional vectors with the length of 100, where the location of Diracs are constrained on integer grid. The spectral measurements are randomly sampled with uniform random distribution, where the zero frequency component was always included. This made the Fourier sensing matrix become a DFT matrix, so we can use basis pursuit using partial DFT sensing matrix. We used the basis pursuit algorithm which was obtained from the original author's homepage [39]. For the proposed method, d is set to be $\lfloor n/2 \rfloor + 1 = 51$. The other hyper-parameters for the proposed method are as follows; $\mu = 10^3$, 200 iterations, $tol = 10^{-4}$ for LMaFit. For fair comparison, we used the same number of iterations and sampling pattern for both basis pursuit and the proposed algorithm. The phase transitions show the success ratio calculated from 300 Monte Carlo trials. Each trial from Monte Carlo simulations is considered as a success when the normalized mean square error (NMSE) is below 10^{-3} . In Fig. 4, the proposed approach provided a sharper transition curve between success and failure than that of the basis pursuit. Furthermore, a transition curve of the proposed method (red dotted line) is higher than that of basis pursuit (blue dotted line).

2) *Piecewise-constant signals*: To generate the piecewise constant signals, we first generated Diracs signal at random locations on integer grid and added steps in between the Diracs. The length of the unknown one-dimensional vector was again set to 100. To avoid boundary effect, the values at the end of both boundaries were set to zeros. As a conventional compressed sensing approach, we employed the 1-D version of l_1 -total variation reconstruction (l_1 -TV) using the split Bregman method [40], which was modified from the original 2-D version of l_1 -TV from author's homepage. We found that the optimal parameters for l_1 -TV were $\mu = 10^3$, $\lambda = 1$, and outer-inner loop iterations of 5 and 40, respectively. The hyper-parameters for the proposed method were the same as before except for the tolerance parameter of LMaFit which was set to $tol = 10^{-3}$. Note that we need $1 - e^{-j\omega}$ weighting for low-rank Hankel matrix completion as a discrete whitening operator for TV signals. The phase transition plots were

calculated using averaged success ratio from 300 Monte Carlo trials. Each trial from Monte Carlo simulations was considered as a success when the NMSE was below 10^{-2} . Because the actual non-zero support of the piecewise constant signals was basically entire domain, the threshold was set larger than the previous Dirac experiments.

As shown in Fig. 5, a transition curve from the proposed method (red dotted line) provided a sharper and improved transition than l_1 total variation approach (blue dotted line). Furthermore, even in the area of success status, there were some unsuccessful recoveries for the case of conventional method, whereas the proposed method succeeded nearly all the times. In Fig. 6, we also illustrated sample recovery results from the same locations in the phase transition diagram, which are at the yellow star marked position in Fig. 5. We observed near perfect reconstruction from the proposed method, whereas severe blurring was observed in l_1 -TV reconstruction.

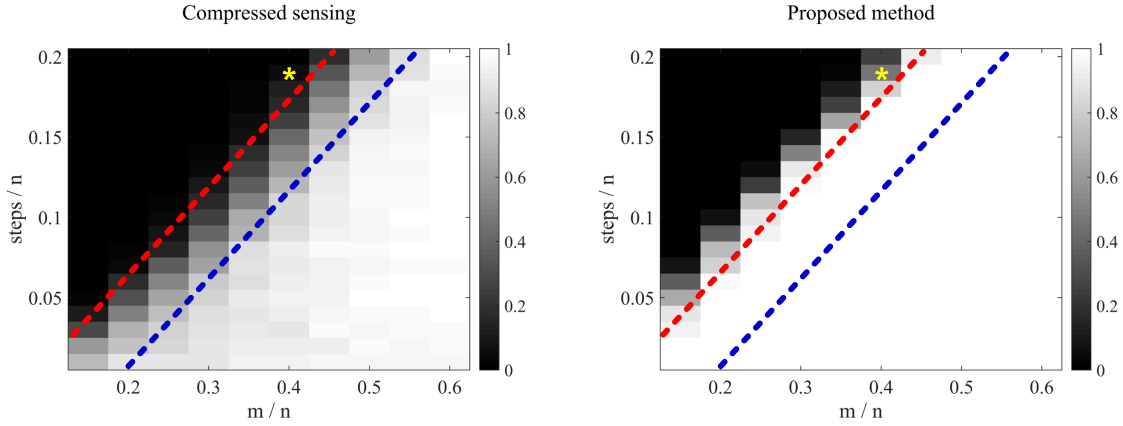


Fig. 5. Phase transition diagrams for piecewise constant signals from m random sampled Fourier samples. The size of target signal (n) is 100 and the annihilating filter size d was set to be 51. The left and right graphs correspond to the phase transition diagram of the l_1 -TV compressed sensing approach and the proposed low-rank interpolation approach, respectively. The success ratio is obtained by the success ratio from 300 Monte Carlo runs. Two transition lines from compressed sensing (blue) and low-rank interpolator (red) are overlaid.

3) *Piecewise-constant signal + Diracs*: We performed additional experiments for reconstruction of a superposition of piecewise constant signal and Dirac spikes. Note that this corresponds to the first derivative of piecewise polynomial with maximum order of 1 (i.e. piecewise constant and linear signals). The goal of this experiment was to verify the capability of recovering piecewise polynomials, but there was no widely used compressed sensing solution for this type of signals; so for a fair comparison, we were interested in recovering their derivatives, because the conventional l_1 -TV approach can be still used for recovering Diracs and piecewise constant signals. In this case, the sparsity level doubles at the Dirac locations when we use l_1 -TV method for this type of signals. Similar sparsity doubling was observed in our approach. More specifically, our method required the derivative operator as a whitening operator, which resulted in the first derivative of Diracs. According to (59), this makes the effective sparsity level doubled. Accordingly, the comparison of l_1 -TV and our low-rank interpolation approach was fair, and the overall phase transition were expected to be inferior compared to those of piecewise constant signals. The simulation environment was set to be same as those of the previous piecewise constant setup except for the signal generation. For signals, we generated equal number of steps and Diracs. When the sparsity is an odd number, the

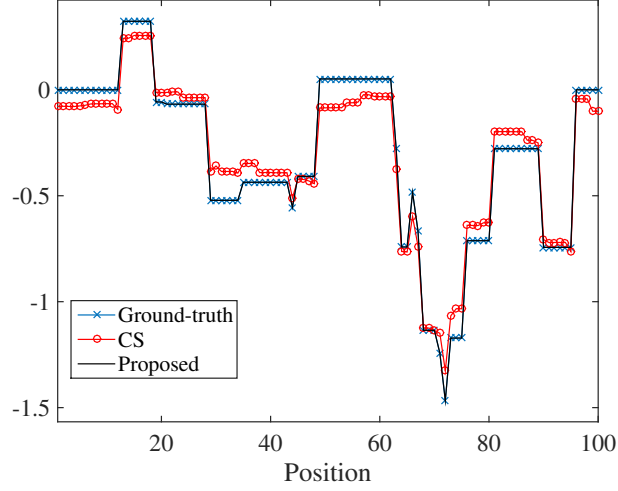


Fig. 6. Sample reconstruction results at the yellow star position in Fig. 5. Ground-truth signal (original), l_1 -TV (compressed sensing) and the proposed method (low-rank interpolator) were illustrated. The parameters for the experiments are: $n = 100$, $d = 51$, $m = 50$ and the number of steps was 19.

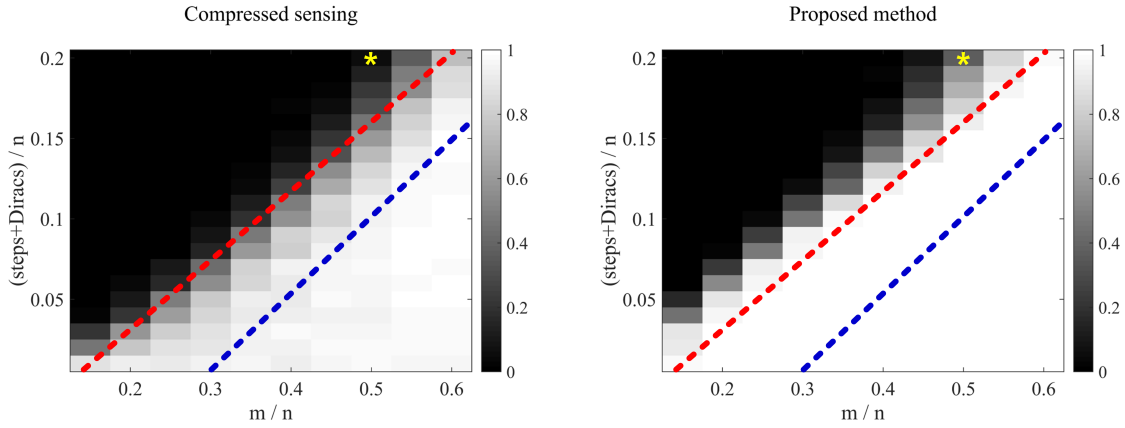


Fig. 7. Phase transition diagrams for recovering super-position of piecewise constant signal and Diracs from m random sampled Fourier samples. The size of target signal (n) is 100 and the annihilating filter size d was set to be 51. The left and right graphs correspond to the phase transition diagram of the l_1 -TV compressed sensing approach and the proposed low-rank interpolation approach, respectively. The success ratio is obtained by the success ratio from 300 Monte Carlo runs. Two transition lines from compressed sensing (blue) and low-rank interpolator (red) are overlaid.

numbers of Diracs was set to the number of steps minus 1.

As shown in Fig. 7, there were much more significant differences between the two approaches. Our algorithm still provided very clear and improved phase transition, whereas the conventional l_1 -TV approach resulted in a very fuzzy and inferior phase transition. In Fig. 8, we also illustrated sample recovery results from the same locations in the phase transition diagram, which are at the yellow star marked position in Fig. 7. The proposed approach provided a near perfect reconstruction, whereas l_1 -TV reconstruction exhibits blurrings. This again confirms the effectiveness of our approach.

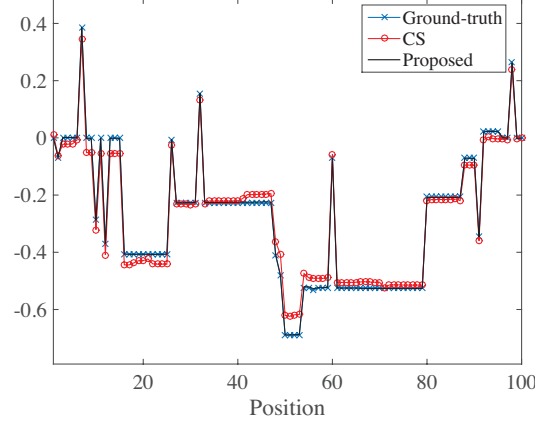


Fig. 8. Sample reconstruction results at the yellow star position in Fig. 7. Ground-truth signal (original), l_1 -TV (compressed sensing) and the proposed method (low-rank interpolator) were illustrated. The parameters for the experiments are: $n = 100$, $d = 51$, $m = 50$ and the number of steps and Diracs were all 10.

B. Noisy Experiments

To verify the noise robustness, We performed experiments using piecewise constant signals by adding the additive complex Gaussian noise to partial Fourier measurements. Fig. 9 showed the recovery performance of the proposed low-rank interpolation method at several signal to noise (SNR) ratios. All setting parameters are same with parameters of previous experiments except the addition of $\lambda = 10^5$. As expected from the theoretical results, the recovery performance was proportional to the noise level.

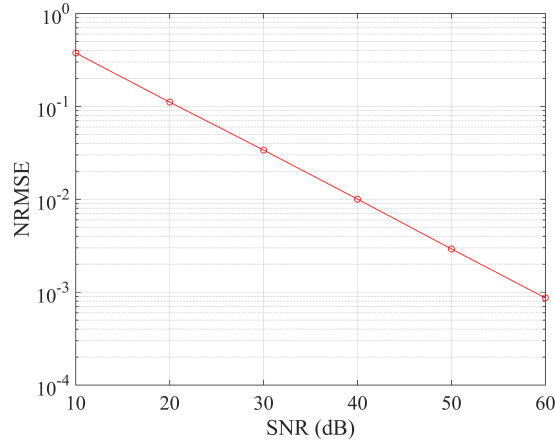


Fig. 9. The reconstruction NMSE plots by the proposed low-rank interpolation scheme at various SNR values. For this simulation, we set the annihilating filter size $d = 51$, $n = 100$, the number of singularity due to steps was 10, and the number of measurements was 50.

VII. CONCLUSION

While the recent theory of compressed sensing (CS) can overcome the Nyquist limit for recovering sparse signals, the existing recovery algorithms require multiple calculations of signal samplings and recovery procedures. To address these issues, this paper developed a new sampling theory that can exploit all of the benefits of the CS using a digital correction filter before the classical reconstruction filter from Nyquist or generalized sampling theory is applied. This breakthrough is founded by the fundamental duality between the sparsity in the primary space and the low-rankness of the structured matrix in the reciprocal spaces, which has theoretical founding in the sampling theory of signals with finite rate of innovations (FRI). We also showed that for the case of r Diracs, the required sampling rate to recover r -Diracs using the proposed method can be reduced to $m \geq \mathcal{O}(r \log^2 n)$, which is an improvement over $m \geq \mathcal{O}(r \log^4 n)$ in the original proof of EMaC [18]. Moreover, our theory was generalized to encompass more general signals with finite rate of innovations, such as piecewise polynomial, splines, and so on. In particular, by restricting the signal class as cardinal splines, the proposed approach provided a natural regularization scheme that can balance the resolution and noise trade-off. The numerical results confirmed that the proposed methods exhibited significantly improved phase transition than the existing CS approaches.

ACKNOWLEDGEMENT

The authors would like to thank Prof. Michael Unser at EPFL for giving an insight into cardinal spline representations.

APPENDIX

APPENDIX A

A. Architecture of Proof

We will follow the original proof by Recht [33], whose proof was inspired by the original work of Gross [19]. The proof is for both Hankel and circulant structured matrices.

1) *Key Lemma:* We first prove the following key lemma that provides the desired property of a dual certificate.

Lemma A.1. *Consider an index set Ω that contains m random indices. Suppose that the sampling operator R_Ω obeys*

$$\frac{n}{m} \left\| P_T R_\Omega P_T - \frac{m}{n} P_T \right\| \leq \frac{1}{2}, \quad \|R_\Omega\|_\infty \leq \frac{8}{3} \beta^{1/2} \log(n) \quad (\text{A.1})$$

For a given $0 < \xi < 1$, if there exists a matrix Y satisfying

$$\|P_T(Y) - UV^*\|_F \leq \xi \sqrt{\frac{9m}{512\beta n \log^2(n)}}, \quad \|P_{T^\perp}(Y)\| < \frac{1}{2} \quad (\text{A.2})$$

then M is the unique solution of (P).

Proof. Suppose $Z \in \ker R_\Omega$ and $X = M + Z$. Then, we have

$$R_\Omega(X - M) = 0.$$

Our goal is to show that for such Z , the nuclear norm inequality still holds, i.e.

$$\|M + Z\|_* \geq \|M\|_*.$$

In this case, by minimizing the nuclear norm, we can find the solution for (P). Now, for $Z \in \ker R_\Omega$, pick U_\perp and V_\perp such that $[U, U_\perp]$ and $[V, V_\perp]$ are unitary matrices and that

$$\langle U_\perp V_\perp^*, P_{T^\perp}(Z) \rangle = \|P_{T^\perp}(Z)\|_*.$$

It then follows

$$\begin{aligned} \|M + Z\|_* &\geq \langle UV^* + U_\perp V_\perp^*, M + Z \rangle \\ &= \|M\|_* + \langle UV^* + U_\perp V_\perp^*, Z \rangle \end{aligned}$$

where we use $\langle U_\perp V_\perp^*, M \rangle = 0$ since U, V are left and right singular vectors of M . If there exists $Y \in \text{range}(R_\Omega)$, we can easily see that

$$\langle Y, Z \rangle = 0, \quad \forall Z \in \ker(R_\Omega).$$

Moreover, we have

$$\begin{aligned} \|M + Z\|_* &\geq \|M\|_* + \langle UV^* + U_\perp V_\perp^* - Y, Z \rangle \\ &= \|M\|_* + \langle UV^* + U_\perp V_\perp^* - P_T(Y) - P_{T^\perp}(Y), P_T(Z) + P_{T^\perp}(Z) \rangle \\ &= \|M\|_* + \langle UV^* - P_T(Y), P_T(Z) \rangle + \langle U_\perp V_\perp^* - P_{T^\perp}(Y), P_{T^\perp}(Z) \rangle \end{aligned}$$

Then, using the following inequalities

$$\langle W, H \rangle \leq \|W\| \|H\|, \tag{A.3}$$

and $\langle U_\perp V_\perp^*, P_{T^\perp}(Z) \rangle = \|P_{T^\perp}(Z)\|_*$, we have

$$\begin{aligned} \|M + Z\|_* &\geq \|M\|_* + \langle UV^* - P_T(Y), P_T(Z) \rangle + \langle U_\perp V_\perp^*, P_{T^\perp}(Z) \rangle - \|P_{T^\perp}(Y)\| \|P_{T^\perp}(Z)\|_* \\ &\geq \|M\|_* - \alpha(Y) \|P_T(Z)\|_F + \beta(Y) \|P_{T^\perp}(Z)\|_* \end{aligned}$$

with

$$\alpha(Y) := \|UV^* - P_T(Y)\|_F, \quad \beta(Y) := 1 - \|P_{T^\perp}(Y)\|.$$

Now, for any $Z \in \ker R_\Omega$, we have

$$0 = \|R_\Omega(Z)\|_F \geq \|R_\Omega P_T(Z)\|_F - \|R_\Omega P_{T^\perp}(Z)\|_F$$

where we used the triangular inequality. Moreover, the following inequalities hold:

$$\|R_\Omega P_T(Z)\|_F^2 = \langle Z, P_T R_\Omega^2 P_T(Z) \rangle \geq \langle P_T(Z), P_T R_\Omega P_T(P_T(Z)) \rangle \geq \frac{m}{2n} \|P_T(Z)\|^2$$

and

$$\|R_\Omega P_{T^\perp}(Z)\|_F \leq \frac{8}{3} \beta^{1/2} \log(n) \|P_{T^\perp}(Z)\|_F$$

where we use (A.1). Consequently, for any $Z \in \ker R_\Omega$,

$$\begin{aligned} \|P_{T^\perp}(Z)\|_F &\geq \frac{3}{8\beta^{1/2} \log(n)} \|R_\Omega P_{T^\perp}(Z)\|_F \\ &\geq \frac{3}{8\beta^{1/2} \log(n)} \|R_\Omega P_T(Z)\|_F \\ &\geq \sqrt{\frac{9m}{128\beta n \log^2(n)}} \|P_T(Z)\|_F \end{aligned} \tag{A.4}$$

Therefore, under the condition (A.2) and (A.1), we have

$$\begin{aligned} \beta(Y) \|P_{T^\perp}(Z)\|_* - \alpha(Y) \|P_T(Z)\|_F &\geq \frac{1}{2} \|P_{T^\perp}(Z)\|_* - \xi \sqrt{\frac{9m}{512\beta n \log^2(n)}} \|P_T(Z)\|_F \\ &\geq \frac{1}{2} (1 - \xi) \|P_{T^\perp}(Z)\|_F + \frac{\xi}{2} \left(\|P_{T^\perp}(Z)\|_F - \sqrt{\frac{9m}{128\beta n \log^2(n)}} \|P_T(Z)\|_F \right) \end{aligned} \tag{A.5}$$

Therefore, using (A.4), for $0 < \xi < 1$, we have

$$\begin{aligned} \|M + Z\|_* &\geq \|M\|_* + \frac{1}{2} (1 - \xi) \|P_{T^\perp}(Z)\|_F \\ &\geq \|M\|_* \end{aligned} \tag{A.6}$$

This concludes the proof. \square

2) *Dual Certification via Golfing Scheme*: Now, the remaining question is how to construct Y . For this, we will again employ a dual certification via “golfing scheme” by Gross [19]. Specifically, partition $1, \dots, m$ into p partitions of size q . Let Ω_j denote the set of indices corresponding to the j -th partition. Note that each partition is independent to one another due to the sampling with replacement. Assume that

$$\frac{n}{q} \left\| P_T R_{\Omega_j} P_T - \frac{q}{n} P_T \right\| \leq \frac{1}{2} \tag{A.7}$$

for all $j \in \{1, \dots, p\}$. Theorem A.6, which will be proven later, shows that this assumption is true with high probability. Define $W_0 = UV^*$ and set

$$Y_k = \frac{n}{q} \sum_{j=1}^k R_{\Omega_j}(W_{j-1}), \quad W_k = UV^* - P_T(Y_k) \tag{A.8}$$

for $k = 1, \dots, p$. Note that the construction makes $W_j \in T$ for all j . Then,

$$\begin{aligned}\|W_k\|_F &= \left\| W_{k-1} - \frac{n}{q} P_T R_{\Omega_k} (W_{k-1}) \right\|_F \\ &= \left\| \left(P_T - \frac{n}{q} P_T R_{\Omega_k} P_T \right) (W_{k-1}) \right\|_F \\ &\leq \frac{1}{2} \|W_{k-1}\|_F\end{aligned}$$

where the second equality comes from $W_{k-1} \in T$. By applying this sequentially, we have

$$\|W_k\|_F \leq 2^{-k} \|W_0\|_F = 2^{-k} \|UV^*\|_F = 2^{-k} \sqrt{r}$$

Since $Y = Y_p$ due to the p -partitioning of $1, \dots, m$, we have

$$\|W_p\|_F = \|UV^* - P_T(Y)\|_F \leq 2^{-p} \sqrt{r} \quad (\text{A.9})$$

Hence, to satisfy the first condition in (A.2), if we use m such that

$$m > \frac{256}{9\xi^2} \beta r \log^2(n), \quad (\text{A.10})$$

then

$$2^{-p} \sqrt{r} \leq \sqrt{\frac{r}{2n}} \iff p \geq \frac{1}{2} \log_2(2n). \quad (\text{A.11})$$

Now, to satisfy the second condition in (A.2), we first need the following inequality, which is true with high probability as will be shown in Theorem A.7:

$$\left\| \left(\frac{n}{q} R_{\Omega_j} - I \right) (W_{j-1}) \right\| \leq \frac{\gamma n \beta \log n}{q} \|W_{j-1}\|_{\mathcal{H}, \infty} \quad (\text{A.12})$$

for $j = 1, \dots, p$, where γ is defined by (A.19) and

$$\|Z\|_{\mathcal{H}, \infty} = \max_k |\langle B_k, Z \rangle|.$$

We further need that

$$\|W_j\|_{\mathcal{H}, \infty} \leq \frac{1}{2} \|W_{j-1}\|_{\mathcal{H}, \infty}$$

which is also true with high probability as will be shown in Corollary A.9. Accordingly, we have

$$\begin{aligned}
\|P_{T^\perp} Y\| = \|P_{T^\perp} Y_p\| &\leq \sum_{j=1}^p \left\| \frac{n}{q} P_{T^\perp} R_{\Omega_j} W_{j-1} \right\| \\
&= \sum_{j=1}^p \left\| P_{T^\perp} \left(\frac{n}{q} R_{\Omega_j} W_{j-1} - W_{j-1} \right) \right\| \\
&= \sum_{j=1}^p \left\| P_{T^\perp} \left(\frac{n}{q} R_{\Omega_j} - I \right) W_{j-1} \right\| \\
&\leq \sum_{j=1}^p \left\| \left(\frac{n}{q} R_{\Omega_j} - I \right) W_{j-1} \right\| \\
&\leq \sum_{j=1}^p \frac{\gamma n \beta \log(n)}{q} \|W_{j-1}\|_{\mathcal{H}, \infty} \\
&= 2 \sum_{j=1}^p 2^{-j} \frac{\gamma n \beta \log(n)}{q} \|W_0\|_{\mathcal{H}, \infty} \\
&\leq \frac{2\gamma c_s \mu_1 r \beta \log(n)}{q}
\end{aligned}$$

where we use $W_{j-1} \in T$ for the first and the second equalities. Therefore, if we set

$$q \geq 4\gamma c_s \mu_1 r \beta \log(n) \tag{A.13}$$

then

$$\|P_{T^\perp} Y\| \leq \frac{1}{2}$$

B. Theorem and Lemmas

One of the most important breakthroughs made by Gross [19] and Recht [33] is to employ *random sampling with replacement* which significantly simplifies the analysis of sampling condition. Specifically, compared to the Bernoulli sampling scheme, each entry index is sampled independently with replacement from the uniform distributions. Even though this allows some elements of a matrix to have repeated samples, Gross showed the following fundamental result that justifies the proof based on random sampling with replacement [19]:

Proposition A.2. *The probability that the nuclear norm heuristic fails when the set of observed entries is sampled uniformly from the collection of sets of size m is less than or equal to the probability that the heuristic fails when m entries are sampled independently with replacement.*

By applying a standard Chernoff bound, Recht bounded the number of repeated entry [33]:

Proposition A.3. [33] *With probability at least $1 - n^{2-2\beta^{1/2}}$,*

$$\|R_\Omega\|_\infty \leq \frac{8}{3} \beta^{1/2} \log(n)$$

for $n \geq 9$ and $\beta > 1$.

One of the most important advantages of the sampling with replacement scheme is that it allows us to use the following non-commutative variant of Bernstein's inequality, which will be used later extensively:

Theorem A.4 (Non-commutative Bernstein Inequality). *Let X_1, \dots, X_L be independent zero mean random matrices of dimension $d_1 \times d_2$. Suppose $\rho_k^2 = \max\{\|E[X_k X_k^*]\|, \|E[X_k^* X_k]\|\}$ and $\|X_k\| \leq M$ almost surely for all k . Then, for any $\tau > 0$,*

$$Pr \left[\left\| \sum_{k=1}^L X_k \right\| > \tau \right] \leq (d_1 + d_2) \exp \left(\frac{-\tau^2/2}{\sum_{k=1}^L \rho_k^2 + M\tau/3} \right) \quad (\text{A.14})$$

Furthermore, if $\tau \leq \frac{1}{M} \sum_{k=1}^L \rho_k^2$, then

$$Pr \left[\left\| \sum_{k=1}^L X_k \right\| > \tau \right] \leq (d_1 + d_2) \exp \left(-\frac{3\tau^2}{8 \sum_{k=1}^L \rho_k^2} \right) \quad (\text{A.15})$$

As a variation of Theorem A.4, we can obtain the following corollary:

Corollary A.5. *Let X_1, \dots, X_L be independent zero mean random matrices of dimension $d_1 \times d_2$. Suppose $\rho_k^2 = \max\{\|E[X_k X_k^*]\|, \|E[X_k^* X_k]\|\}$ and $\|X_k\| \leq M$ almost surely for all k . Then, for $\beta > 1$ and $n \geq 3$, we have*

$$Pr \left[\left\| \sum_{k=1}^L X_k \right\| > \tau_0 \right] \leq (d_1 + d_2) n^{-\beta} \quad (\text{A.16})$$

where

$$\tau_0 = \frac{M}{3} \left(1 + \sqrt{1 + \frac{18R}{M^2}} \right) \beta \log(n), \quad R := \sum_{k=1}^L \rho_k^2. \quad (\text{A.17})$$

Proof. Let $R := \sum_{k=1}^L \rho_k^2$. Consider the parabolic equation

$$f(\tau) = \frac{\tau^2}{2\beta \log(n)} - \frac{M}{3}\tau - R.$$

Note that $f(\tau)$ has both positive and negative roots. Let τ_+ denote the positive root. Then, by setting $\tau = \tau_+$, (A.14) can be simplified as

$$Pr \left[\left\| \sum_{k=1}^L X_k \right\| > \tau_+ \right] \leq (d_1 + d_2) n^{-\beta}.$$

Furthermore, for any $\tau_0 \geq \tau_+$, $f(\tau_0) \geq 0$ and the argument within the exponent in (A.14) becomes more negative; so we can still use the bound:

$$Pr \left[\left\| \sum_{k=1}^L X_k \right\| > \tau_0 \right] \leq (d_1 + d_2) n^{-\beta}.$$

Therefore, the remaining issue is to find $\tau_0 \geq \tau_+$ that has a simple expression. Using the formulae for the root of second order polynomial, we have

$$\tau_+ = \frac{M}{3} \beta \log(n) + \sqrt{\left(\frac{M}{3} \beta \log(n) \right)^2 + 2R\beta \log(n)}$$

Because $\log^2(n) \geq \log(n)$ for $n \geq 3$ and $\beta^2 \geq \beta$ for $\beta > 1$, we have

$$\begin{aligned}\tau_+ &\leq \frac{M}{3}\beta \log(n) + \sqrt{\left(\frac{M}{3}\beta \log(n)\right)^2 + 2R\beta^2 \log^2(n)} \\ &= \frac{M}{3}\beta \log(n) \left(1 + \sqrt{1 + \frac{18R}{M^2}}\right) \\ &:= \tau_0\end{aligned}$$

This concludes the proof. \square

Using the non-commutative Bernstein inequality, here we provide the required theorem and lemma for the dual certification.

Theorem A.6. *Suppose Ω is a set of coefficients of size m sampled independently and uniformly with replacement. Then, for all $\beta > 1$,*

$$\frac{n}{m} \left\| P_T R_\Omega P_T - \frac{m}{n} P_T \right\| \leq \sqrt{\frac{16\mu_0 c_s r \beta \log(n)}{3m}} \quad (\text{A.18})$$

with probability at least $1 - 2n^{1-\beta}$ provided that $m > \frac{16}{3} c_s \mu_0 r \beta \log(n)$.

Proof. For any matrix $Z \in \mathcal{H}(n, d)$ (resp. $Z \in \mathcal{H}_c(n, d)$),

$$P_T R_\Omega P_T(Z) = \sum_{k=1}^m \langle B_k, P_T(Z) \rangle P_T(B_k) = \sum_{k=1}^m \langle P_T(B_k), Z \rangle P_T(B_k)$$

Let $\mathcal{F}_k := P_T R_k P_T - \frac{1}{n} P_T$, such that $P_T R_\Omega P_T - \frac{m}{n} P_T = \sum_{k=1}^m \mathcal{F}_k$. It is easy to see $\mathbb{E}(\mathcal{F}_k(Z)) = 0$ for any $Z \in \mathcal{H}(n, d)$ (resp. $Z \in \mathcal{H}_c(n, d)$), so we have $\mathbb{E}(\mathcal{F}_k) = 0$. Next, for any $Z \in \mathcal{H}(n, d)$ (resp. $Z \in \mathcal{H}_c(n, d)$), we have

$$\begin{aligned}P_T R_k P_T(Z) &= \langle B_k, P_T(Z) \rangle P_T(B_k) \\ (P_T R_k P_T)^2(Z) &= (P_T R_k P_T) \langle B_k, P_T(Z) \rangle P_T(B_k) \\ &= \langle B_k, P_T(Z) \rangle \langle B_k, P_T(B_k) \rangle P_T(B_k) \\ &= \langle B_k, P_T(B_k) \rangle P_T R_k P_T(Z) \\ &\leq \frac{2c_s \mu_0 r}{n} P_T R_k P_T(Z)\end{aligned}$$

where the last inequality comes from (97). This further gives

$$\|P_T R_k P_T\| = |\langle B_k, P_T(B_k) \rangle|.$$

For positive semi-definite matrices A and B , we have $\|A - B\| \leq \max\{\|A\|, \|B\|\}$, so we have

$$\begin{aligned}\|\mathcal{F}_k\| &\leq \max\{\|P_T R_k P_T\|, \|\frac{1}{n} P_T\|\} \leq \max\{|\langle B_k, P_T(B_k) \rangle|, \frac{1}{n}\} \\ &\leq c_s \mu_0 r \frac{2}{n}\end{aligned}$$

Second,

$$\begin{aligned}\rho_k^2 = \|\mathbb{E}(\mathcal{F}_k^* \mathcal{F}_k)\| &= \|\mathbb{E}(P_T R_k P_T)^2 - (\mathbb{E}(P_T R_k P_T))^2\| \\ &\leq \max\{\|\mathbb{E}(P_T R_k P_T)^2\|, \|(\mathbb{E}(P_T R_k P_T))^2\|\}\end{aligned}$$

We further note that

$$\begin{aligned}\mathbb{E}(P_T R_k P_T) &= \frac{1}{n} P_T \\ \|\mathbb{E}(P_T R_k P_T)^2\| &\leq c_s \mu_0 r \frac{2}{n} \|\mathbb{E}(P_T R_k P_T)\| = c_s \mu_0 r \frac{2}{n^2}\end{aligned}$$

Therefore, from the noncommutative Bernstein inequality, we have

$$\begin{aligned}Pr\left[\|P_T R_\Omega P_T - \frac{m}{n} P_T\| > \tau \frac{m}{n}\right] &\leq (n+1) \exp\left(-\frac{3\tau^2 m^2 / (n^2)}{8m\mu_0 r \frac{2}{n^2}}\right) \\ &= (n+1) \exp\left(-\frac{3\tau^2 m}{16c_s \mu_0 r}\right)\end{aligned}$$

Therefore, if we set $\tau = \sqrt{\frac{16\mu_0 c_s r \beta \log(n)}{3m}}$, we have

$$\begin{aligned}Pr\left[\frac{n}{m} \|P_T R_\Omega P_T - \frac{m}{n} P_T\| > \tau\right] &\leq (n+1) \exp(-\beta \log(n)) \\ &= (n+1) n^{-\beta} < 2n^{1-\beta}.\end{aligned}$$

under the constraint $\tau \leq \frac{1}{M} \sum_{k=1}^n \rho_k^2$, which can be represented as

$$c_s \mu_0 r \frac{2}{n} \sqrt{\frac{16\mu_0 c_s r \beta \log(n)}{3m}} \leq c_s \mu_0 r \frac{2}{n}.$$

Hence, we need $m \geq \frac{16}{3} c_s \mu_0 r \beta \log(n)$. This concludes the proof. \square

Theorem A.7. *Let Ω be a set of coefficients of size m sampled independently and uniformly with replacement and let Z be any matrix in $\mathcal{H}(n, d)$ (resp. $\mathcal{H}_c(n, d)$). Assume without loss of generality that $n - d + 1 \geq d$. Then, for all $\beta > 1$,*

$$\left\| \left(\frac{n}{m} R_\Omega - I \right) (Z) \right\| \leq \frac{\gamma n \beta \log(n)}{m} \|Z\|_{\mathcal{H}, \infty}$$

where

$$\gamma = \frac{2}{3} \left(1 + \sqrt{1 + \frac{3}{2} \alpha(n, d)} \right) \quad (\text{A.19})$$

with probability at least $1 - 2n^{1-\beta}$.

Proof. Let

$$\mathcal{F}_k(Z) := n\langle B_k, Z \rangle B_k - Z.$$

Then, $\left(\frac{n}{m}R_\Omega - I\right)(Z) = \frac{1}{m} \sum_{k=1}^m \mathcal{F}_k(Z)$. Moreover,

$$\begin{aligned} \mathbb{E}[\mathcal{F}_k(Z)] &= \mathbb{E}[n\langle B_k, Z \rangle B_k - Z] \\ &= \sum_{k=1}^n \langle B_k, Z \rangle B_k - Z = 0 \end{aligned}$$

and

$$\begin{aligned} \frac{1}{m} \|\mathcal{F}_k(Z)\| &\leq \frac{1}{m} (\|n\langle B_k, Z \rangle B_k\| + \|Z\|) \\ &\leq \frac{2}{m} \|n\langle B_k, Z \rangle B_k\| \\ &\leq \frac{2n}{m} \|Z\|_{\mathcal{H}, \infty} \|B_k\| \\ &\leq \frac{2n}{m} \|Z\|_{\mathcal{H}, \infty} \end{aligned}$$

Furthermore,

$$\begin{aligned} \frac{1}{m^2} \|\mathbb{E}[\mathcal{F}_k^*(Z) \mathcal{F}_k(Z)]\| &= \|n^2 \mathbb{E}[\langle B_k, Z \rangle^2 B_k^* B_k] - Z^* Z\| \\ &= \frac{1}{m^2} \max\{\|n \sum_{k=1}^n \langle B_k, Z \rangle^2 B_k^* B_k\|, \|Z^* Z\|\} \\ &\leq \frac{n}{m^2} \|Z\|_{\mathcal{H}, \infty}^2 \sum_{k=1}^n \|B_k^* B_k\| \\ &\leq \frac{n}{m^2} \alpha(n, d) \|Z\|_{\mathcal{H}, \infty}^2 \end{aligned}$$

A similar calculation for $\|\mathbb{E}[\mathcal{F}_k(Z) \mathcal{F}_k(Z)^*]\|$ results in the same upper bound

$$\frac{1}{m^2} \|\mathbb{E}[\mathcal{F}_k(Z) \mathcal{F}_k^*(Z)]\| \leq \frac{n}{m^2} \alpha(n, d) \|Z\|_{\mathcal{H}, \infty}^2.$$

Hence, to use Corollary A.5, set

$$M := \frac{2n}{m} \|Z\|_{\mathcal{H}, \infty}, \quad R := \frac{n}{m^2} \alpha(n, d) \|Z\|_{\mathcal{H}, \infty}^2$$

Then, we have

$$\begin{aligned} \Pr \left[\left\| \left(\frac{n}{m} R_\Omega - I \right) (Z) \right\| \geq \tau_0 \right] &\leq \Pr \left[\left\| \frac{1}{m} \sum_{k=1}^m \mathcal{F}_k(Z) \right\| \geq \tau_0 \right] \\ &\leq (n+1)n^{-\beta} \leq 2n^{1-\beta} \end{aligned}$$

where

$$\begin{aligned}\tau_0 &= \frac{2n}{3m}\beta\|Z\|_{\mathcal{H},\infty}\log(n)\left(1 + \sqrt{1 + \frac{9}{2n}\alpha(n,d)}\right) \\ &\leq \frac{2n}{3m}\beta\|Z\|_{\mathcal{H},\infty}\log(n)\left(1 + \sqrt{1 + \frac{3}{2}\alpha(n,d)}\right)\end{aligned}$$

where we use the assumption $n \geq 3$ to obtain an upper bound. Therefore, by defining a new threshold

$$\tau_1 = \frac{\gamma n \beta \log(n)}{m} \|Z\|_{\mathcal{H},\infty}$$

with

$$\gamma = \frac{2}{3} \left(1 + \sqrt{1 + \frac{3}{2}\alpha(n,d)}\right)$$

we conclude the proof. \square

Lemma A.8. *Suppose Ω is a set of coefficients of size m sampled independently and uniformly with replacement and let $Z \in T$ be a fixed structured matrix in $\mathcal{H}(n, d)$ (resp. $\mathcal{H}_c(n, d)$). Assume without loss of generality that $n - d + 1 \geq d$. Then, for all $\beta > 1$,*

$$\left\| \frac{n}{m} P_T R_\Omega(Z) - Z \right\|_{\mathcal{H},\infty} \leq \sqrt{\frac{32c_s\beta\mu_0 r \log(n)}{3m}} \|Z\|_{\mathcal{H},\infty}$$

with probability at least $1 - 2n^{1-\beta}$ provided that $m > \frac{32}{3}c_s\beta\mu_0 \log(n)$.

Proof. This lemma can be proven using standard Bernstein inequality, which can be easily obtained by considering scalar random variables (i.e. $n = n_2 = 1$) in the noncommutative Bernstein inequality. Let

$$\mathcal{F}_k(Z) := n\langle B_k, Z \rangle P_T(B_k) - Z.$$

For each basis index c , we sample k uniformly at random to define a scalar random variable

$$\xi_c := \langle B_c, \mathcal{F}_k(Z) \rangle.$$

Then,

$$\begin{aligned}\mathbb{E}[\xi_c] &= n\mathbb{E}[\langle B_c, P_T(B_k) \rangle \langle B_k, Z \rangle] - \langle B_c, Z \rangle \\ &= \sum_{k=1}^n \langle B_c, P_T(B_k) \rangle \langle B_k, Z \rangle - \langle B_c, Z \rangle \\ &= \langle B_c, P_T(Z) \rangle - \langle B_c, Z \rangle \\ &= 0\end{aligned}$$

where in the last equalities we use $Z \in T$. Moreover, we have

$$\begin{aligned}
|\xi_c| &= |\langle B_c, \mathcal{F}_k(Z) \rangle| = |\langle B_c, n\langle B_k, Z \rangle P_T(B_k) - Z \rangle| \\
&\leq 2|\langle B_c, n\langle B_k, Z \rangle P_T(B_k) \rangle| \\
&\leq 2n\|Z\|_{\mathcal{H},\infty} |\langle B_c, P_T(B_k) \rangle| \\
&\leq 4c_s\mu_0r\|Z\|_{\mathcal{H},\infty}
\end{aligned}$$

In addition, we have

$$\begin{aligned}
\mathbb{E}[n^2\langle B_k, Z \rangle^2 \langle B_c, P_T(B_k) \rangle^2] &= n \sum_{k=1}^n \langle P_T(B_c), B_k \rangle^2 \langle B_k, Z \rangle^2 \\
&\leq n\|Z\|_{\mathcal{H},\infty}^2 \sum_{k=1}^n \langle P_T(B_c), B_k \rangle^2 \\
&\leq n\|Z\|_{\mathcal{H},\infty}^2 \|P_T(B_c)\|_F^2 \\
&\leq n\|Z\|_{\mathcal{H},\infty}^2 |\langle B_c, P_T(B_c) \rangle| \\
&= 2c_s\mu_0r\|Z\|_{\mathcal{H},\infty}^2
\end{aligned}$$

Accordingly,

$$\begin{aligned}
\mathbb{E}[\xi_c^2] &= \mathbb{E}[n^2\langle P_T(B_k), Z \rangle^2 \langle B_c, P_T(B_k) \rangle^2] - \langle B_c, Z \rangle^2 \\
&\leq 4c_s\mu_0r\|Z\|_{\mathcal{H},\infty}^2
\end{aligned}$$

Since $\langle B_c, \frac{n}{m}P_T R_\Omega(Z) - Z \rangle$ is identically distributed to $\frac{1}{m} \sum_{k=1}^m \xi_c^{(k)}$, where $\xi_c^{(k)}$ are i.i.d. copies of ξ_c , we have by Bernstein's inequality :

$$\begin{aligned}
Pr \left[\frac{1}{m} \sum_{k=1}^m \xi_c^{(k)} > \tau \right] &\leq Pr \left[\sum_{k=1}^m \xi_c^{(k)} > m\tau \right] \\
&\leq 2 \exp \left(-\frac{3\tau^2 m}{32c_s\mu_0r\|Z\|_{\mathcal{H},\infty}^2} \right)
\end{aligned}$$

Hence, using the union bound we have

$$\begin{aligned}
Pr \left[\left\| \frac{n}{m} P_T R_\Omega(Z) - Z \right\|_{\mathcal{H},\infty} > \tau \right] &= 1 - \prod_c Pr \left[\frac{1}{m} \sum_{k=1}^m \xi_c^{(k)} \leq \tau \right] \\
&\leq \sum_c Pr \left[\frac{1}{m} \sum_{k=1}^m \xi_c^{(k)} > \tau \right] \\
&\leq 2n \exp \left(-\frac{3\tau^2 m}{32c_s\mu_0r\|Z\|_{\mathcal{H},\infty}^2} \right) \\
&\leq 2n \exp(-\beta \log(n)) = 2n^{1-\beta}
\end{aligned}$$

where we set $\tau = \sqrt{\frac{32c_s\beta\mu_0r\log(n)}{3m}}\|Z\|_{\mathcal{H},\infty}$. This should hold under the constraint:

$$m\tau \leq m\|Z\|_{\mathcal{H},\infty}$$

which provides us

$$m > \frac{32}{3}c_s\beta\mu_0\log(n).$$

This concludes the proof. \square

Corollary A.9. *Suppose Ω is a set of coefficients of size m sampled independently and uniformly with replacement and let $Z \in T$ be a fixed structured matrix in $\mathcal{H}(n, d)$ (resp. $\mathcal{H}_c(n, d)$). Then, for all $\beta > 1$,*

$$\left\| \frac{n}{m}P_T R_\Omega(Z) - Z \right\|_{\mathcal{H},\infty} \leq \frac{1}{2}\|Z\|_{\mathcal{H},\infty}$$

with probability at least $1 - 2n^{1-\beta}$ provided that $m > \frac{128}{3}c_s\beta\mu_0r\log(n)$.

Proof. From Lemma A.8, we need $m > \frac{128}{3}c_s\beta\mu_0r\log(n)$, which satisfies the sampling requirement $\frac{32}{3}c_s\beta\mu_0\log(n)$ because of $r \geq 1$. This concludes the proof. \square

C. Sample Number and Failure Rate

Now, we are ready to calculate the total sample numbers. First, from (A.11), we need $p \geq \frac{3}{4}\log(2n)$ segments, where we use the upper bound $\frac{3}{4}\log(2n) \geq \frac{1}{2}\log_2(2n)$. In addition, using (A.13), we have $q \geq 4\gamma c_s\mu_1r\beta\log n$ to make the right hand size value to $\frac{1}{2}$, which leads to

$$m > 3\gamma c_s\mu_1r\beta\log^2(2n).$$

For Theorem A.6, we need $q > \frac{16}{3}c_s\mu_0r\beta\log(n)$, so we have

$$m > 4\beta c_s\mu_0r\log^2(2n).$$

Finally, for Lemma A.8, we need $q > \frac{128}{3}\beta c_s\mu_0r\log(n)$, which leads to

$$m > 32\beta c_s\mu_0r\log^2(2n)$$

Finally, from (A.10), we need

$$m > \frac{256}{9\xi^2}\beta r\log^2(n)$$

for a constant $0 < \xi < 1$. By setting $\xi = \sqrt{8}/3$, this becomes

$$m > 32\beta r\log^2(n)$$

By combining all the bounds, we need

$$m > 32\beta c_s \max\{\mu_0, \frac{3}{32}\gamma\mu_1\} r \log^2(2n).$$

Next, due to Proposition A.3, the failure rate for the upper bound of the duplication is $n^{2-2\beta^{1/2}}$. Now, taking the union bounds for the failure rate in the above table for all $j = 1, \dots, p$, we can show that all of the events holds with probability at least

$$1 - \frac{3}{2} \log(n) n^{1-\beta} - n^{2-2\beta^{1/2}}.$$

APPENDIX B

Let $H := \hat{M} - M$ denote the reconstruction error. Then, we are interested in finding its upper bound:

$$\|H\|_F^2 = \|R_\Omega(H)\|_F^2 + \|R_{\Omega^c}(H)\|_F^2$$

Bounding the first quantity is easy. Using the triangular inequality, we have

$$\|R_\Omega(H)\|_F = \|R_\Omega(\hat{M}) - R_\Omega(M)\|_F \leq \|R_\Omega(\hat{M}) - R_\Omega(Y)\|_F + \|R_\Omega(Y) - R_\Omega(M)\|_F \leq 2\delta \quad (\text{A.20})$$

since M is feasible. Hence, we need to bound $\|R_{\Omega^c}(H)\|_F$. Using the Pythagorean identity, we have

$$\|R_{\Omega^c}(H)\|_F = \|P_T R_{\Omega^c}(H)\|_F + \|P_{T^\perp} R_{\Omega^c}(H)\|_F \quad (\text{A.21})$$

To derive a bound on $\|P_T R_{\Omega^c}(H)\|_F$, note that $R_{\Omega^c}(H) \in \ker R_\Omega$. Consequently, by using (A.4) with $Z = R_{\Omega^c}(H)$, we have

$$\|P_{T^\perp}(R_{\Omega^c}(H))\|_F \geq \sqrt{\frac{9m}{128\beta n \log^2(n)}} \|P_T(R_{\Omega^c}(H))\|_F$$

Therefore, (A.21) can be bounded by

$$\|R_{\Omega^c}(H)\|_F \leq \left(1 + \sqrt{\frac{9m}{128\beta n \log^2(n)}}\right) \|P_{T^\perp} R_{\Omega^c}(H)\|_F \quad (\text{A.22})$$

Hence, the remaining step is to bound $\|P_{T^\perp} R_{\Omega^c}(H)\|_F$. Using (A.6) with $Z = R_{\Omega^c}(H)$, we have

$$\|M + R_{\Omega^c}(H)\|_* \geq \|M\|_* + \frac{1}{2}(1 - \xi) \|P_{T^\perp} R_{\Omega^c}(H)\|_F$$

Since \hat{M} is a feasible solution for P_{noisy} , we have

$$\|M\|_* \geq \|\hat{M}\|_* = \|M + H\|_*$$

Accordingly, we have

$$\begin{aligned} \|M\|_* &\geq \|M + R_{\Omega^c}(H)\|_* - \|R_\Omega(H)\|_* \\ &\geq \|M\|_* + \frac{1}{2}(1 - \xi) \|P_{T^\perp} R_{\Omega^c}(H)\|_F - \|R_\Omega(H)\|_* \end{aligned}$$

Therefore, we have

$$\|P_{T^\perp} R_{\Omega^c}(H)\|_F \leq \frac{2}{1-\xi} \|R_\Omega(H)\|_* \leq \frac{2r}{1-\xi} \|R_\Omega(H)\|_F \leq \frac{4r}{1-\xi} \delta$$

where the last inequality comes from (A.20). Therefore, we have

$$\|\hat{M} - M\|_F^2 = \|H\|_F^2 \leq 2\delta \left[1 + \left(1 + \sqrt{\frac{9m}{128\beta n \log^2(n)}} \right) \frac{2r}{1-\xi} \right] \quad (\text{A.23})$$

Using the required sampling rate in (99) with $\xi = \sqrt{8}/3$, we have

$$\|\hat{M} - M\|_F^2 = \|H\|_F^2 \leq 2\delta \left[1 + \left(1 + \frac{3}{2} \sqrt{rc_s \max\{\mu_0, \frac{3}{32}\gamma\mu_1\}} \right) \frac{2r}{1-\sqrt{8}/3} \right] \quad (\text{A.24})$$

This concludes the proof.

REFERENCES

- [1] D. Donoho, "Compressed sensing," *IEEE Trans. on Information Theory*, vol. 52, no. 4, pp. 1289–1306, April 2006.
- [2] E. Candès, J. Romberg, and T. Tao, "Robust uncertainty principles: Exact signal reconstruction from highly incomplete frequency information," *IEEE Trans. on Information Theory*, vol. 52, no. 2, pp. 489–509, Feb. 2006.
- [3] E. Candès and T. Tao, "Decoding by linear programming," *IEEE Trans. on Information Theory*, vol. 51, no. 12, pp. 4203–4215, Dec. 2005.
- [4] J. Tropp, "Just Relax: convex programming methods for identifying sparse signals in noise," *IEEE Trans. on Information Theory*, vol. 52, no. 3, pp. 1030–1051, March 2006.
- [5] I. Gorodnitsky and B. Rao, "Sparse signal reconstruction from limited data using FOCUSS: Re-weighted minimum norm algorithm," *IEEE Trans. on Signal Processing*, vol. 45, no. 3, pp. 600–616, 1997.
- [6] E. Candès, M. Wakin, and S. Boyd, "Enhancing sparsity by reweighted l_1 minimization," *Journal of Fourier Analysis and Applications*, vol. 14, no. 5, pp. 877–905, 2008.
- [7] S. S. Chen, D. L. Donoho, and M. A. Saunders, "Atomic decomposition by basis pursuit," *SIAM Journal on Scientific computing*, vol. 20, no. 1, pp. 33–61, 1999.
- [8] S. Ji, Y. Xue, and L. Carin, "Bayesian compressive sensing," *IEEE Trans. on Signal Processing*, vol. 56, no. 6, pp. 2346–2356, 2008.
- [9] D. Wipf and B. Rao, "Sparse Bayesian learning for basis selection," *IEEE Trans. on Signal Processing*, vol. 52, no. 8, pp. 2153–2164, 2004.
- [10] H. H. Bauschke and P. L. Combettes, *Convex analysis and monotone operator theory in Hilbert spaces*. Springer Science & Business Media, 2011.
- [11] M. Vetterli, P. Marziliano, and T. Blu, "Sampling signals with finite rate of innovation," *Signal Processing, IEEE Transactions on*, vol. 50, no. 6, pp. 1417–1428, 2002.
- [12] P. L. Dragotti, M. Vetterli, and T. Blu, "Sampling moments and reconstructing signals of finite rate of innovation: Shannon meets Strang–Fix," *IEEE Trans. on Signal Processing*, vol. 55, no. 5, pp. 1741–1757, 2007.
- [13] I. Maravic and M. Vetterli, "Sampling and reconstruction of signals with finite rate of innovation in the presence of noise," *IEEE Trans. on Signal Processing*, vol. 53, no. 8, pp. 2788–2805, 2005.
- [14] R. G. Baraniuk, E. Candès, R. Nowak, and M. Vetterli, "Compressive sampling," *IEEE Signal Processing Magazine*, vol. 25, no. 2, pp. 12–13, 2008.
- [15] M. F. Duarte and R. G. Baraniuk, "Spectral compressive sensing," *Applied and Computational Harmonic Analysis*, vol. 35, no. 1, pp. 111–129, 2013.
- [16] E. J. Candès and C. Fernandez-Granda, "Towards a mathematical theory of super-resolution," *Communications on Pure and Applied Mathematics*, vol. 67, no. 6, pp. 906–956, 2014.

- [17] G. Tang, B. N. Bhaskar, P. Shah, and B. Recht, "Compressed sensing off the grid," *IEEE Transactions on Information Theory*, vol. 59, no. 11, pp. 7465–7490, 2013.
- [18] Y. Chen and Y. Chi, "Robust spectral compressed sensing via structured matrix completion," *IEEE Trans. on Information Theory*, vol. 60, no. 10, pp. 6576 – 6601, 2014.
- [19] D. Gross, "Recovering low-rank matrices from few coefficients in any basis," *IEEE Trans. on Information Theory*, vol. 57, no. 3, pp. 1548–1566, 2011.
- [20] M. Unser, "Sampling-50 years after shannon," *Proceedings of the IEEE*, vol. 88, no. 4, pp. 569–587, 2000.
- [21] M. Unser and A. Aldroubi, "A general sampling theory for nonideal acquisition devices," *IEEE Transactions on Signal Processing*, vol. 42, no. 11, pp. 2915–2925, 1994.
- [22] D. Lee, K. H. Jin, E. Y. Kim, S.-H. Park, and J. C. Ye, "Acceleration of MR parameter mapping using annihilating filter-based low rank Hankel matrix (ALOHA)," *Magn. Reson. Med (in press)*, 2015.
- [23] J. Lee, K. H. Jin, and J. C. Ye, "Reference-free single-pass EPI Nyquist ghost correction using annihilating filter-based low rank Hankel structured matrix," *Magn. Reson. Med (in press)*, 2015.
- [24] K. H. Jin and J. C. Ye, "Annihilating filter based low rank hankel matrix approach for image inpainting," *IEEE Trans. on Image Processing*, vol. 24, no. 11, pp. 3498 – 3511, 2015.
- [25] J. Min, L. Carlini, M. Unser, S. Manley, and J. C. Ye, "Fast live cell imaging at nanometer scale using annihilating filter based low rank Hankel matrix approach," in *SPIE Optical Engineering+ Applications*. International Society for Optics and Photonics, 2015, pp. 95 970V–95 970V.
- [26] K. H. Jin and J. C. Ye, "Sparse + low rank decomposition of annihilating filter-based Hankel matrix for impulse noise removal," *arXiv preprint arXiv:1510.05559*, 2015.
- [27] M. Unser, P. D. Tafti, and Q. Sun, "A unified formulation of Gaussian versus sparse stochastic processes–Part I: Continuous-domain theory," *IEEE Trans. on Information Theory*, vol. 60, no. 3, pp. 1945–1962, 2014.
- [28] M. Unser, P. Tafti, A. Amini, and H. Kirshner, "A unified formulation of Gaussian versus sparse stochastic processes–Part II: Discrete-domain theory," *IEEE Trans. on Information Theory*, vol. 60, no. 5, pp. 3036–3051, 2014.
- [29] H. Krim and M. Viberg, "Two decades of array signal processing research: the parametric approach," *IEEE Signal Processing Magazine*, vol. 13, no. 4, pp. 67–94, 1996.
- [30] Z.-P. Liang and P. C. Lauterbur, *Principles of magnetic resonance imaging*. SPIE Optical Engineering Press, 2000.
- [31] Y. Hua and T. K. Sarkar, "Matrix pencil method for estimating parameters of exponentially damped/undamped sinusoids in noise," *IEEE Trans. on Acoustic Speech and Signal Processing*, vol. 38, no. 5, pp. 814–824, 1990.
- [32] M. Unser and P. D. Tafti, *An introduction to sparse stochastic processes*. Cambridge University Press, 2010.
- [33] B. Recht, "A simpler approach to matrix completion," *The Journal of Machine Learning Research*, vol. 12, pp. 3413–3430, 2011.
- [34] E. J. Candes and Y. Plan, "Matrix completion with noise," *Proceedings of the IEEE*, vol. 98, no. 6, pp. 925–936, 2010.
- [35] M. Signoretto, V. Cevher, and J. A. Suykens, "An SVD-free approach to a class of structured low rank matrix optimization problems with application to system identification," in *IEEE Conf. on Decision and Control*, 2013.
- [36] Z. Wen, W. Yin, and Y. Zhang, "Solving a low-rank factorization model for matrix completion by a nonlinear successive over-relaxation algorithm," *Math. Prog. Comp.*, vol. 4, no. 4, pp. 333–361, 2012.
- [37] N. Srebro, "Learning with matrix factorizations," Ph.D. dissertation, Dept. of Elect. Eng. and Comput. Sci., MIT, MA, 2004.
- [38] S. Boyd, N. Parikh, E. Chu, B. Peleato, and J. Eckstein, "Distributed optimization and statistical learning via the alternating direction method of multipliers," *Found. Trends in Mach. Learn.*, vol. 3, no. 1, pp. 1–122, 2011.
- [39] E. Van Den Berg and M. P. Friedlander, "Probing the Pareto frontier for basis pursuit solutions," *SIAM Journal on Scientific Computing*, vol. 31, no. 2, pp. 890–912, 2008.
- [40] T. Goldstein and S. Osher, "The split Bregman method for l_1 -regularized problems," *SIAM Journal on Imaging Sciences*, vol. 2, no. 2, pp. 323–343, 2009.